

THE MELT POOL SIZE AND ASSOCIATED EFFECTS ON BEAD GEOMETRY IN WAAM

M.Tech. Thesis

By

Prabhat Mishra



**DISCIPLINE OF MECHANICAL ENGINEERING
INDIAN INSTITUTE OF TECHNOLOGY
INDORE**

June 2022

**THE MELT POOL SIZE AND
ASSOCIATED EFFECTS ON BEAD
GEOMETRY IN WAAM**

A THESIS

*Submitted in partial fulfilment of the
requirements for the award of the degree*

of

Master of Technology

In

Mechanical engineering

with specialization in

Production and Industrial Engineering

by

Prabhat Mishra



**DISCIPLINE OF MECHANICAL ENGINEERING
INDIAN INSTITUTE OF TECHNOLOGY
INDORE**

June 2022



INDIAN INSTITUTE OF TECHNOLOGY INDORE

CANDIDATE'S DECLARATION

I hereby certify that the work which is being presented in the thesis entitled **The melt pool size and associated effects on bead geometry in WAAM** in the partial fulfillment of the requirements for the award of the degree of **MASTER OF TECHNOLOGY** and submitted in the **DISCIPLINE OF Mechanical Engineering, Indian Institute of Technology Indore**, is an authentic record of my own work carried out during the period from July 2020 to May 2022 under the supervision of Dr Yuvraj Kumar Madhukar, Assistant Professor in the Department of Mechanical Engineering

The matter presented in this thesis has not been submitted by me for the award of any other degree at this or any other institute.

(Prabhat Mishra)

----- This is to certify that the above statement made by the candidate is correct to the best of my knowledge.

28/05/22

(Dr. Yuvraj Kumar Madhukar)

----- **Prabhat Mishra** has completed his M.Tech. Viva held on **DATE**

28/05/22

Signature of Thesis Supervisor
Date of Signature

30/05/22

Signature of Convener, DPGC
Date of Signature

Name and signature of PSPC Member 1 with date: (Dr Hemant Borkar)

28/5/2022

Date Of Signature

Name and signature of PSPC Member 2 with date: (Dr Kazi Sabiruddin)

29/05/2022

Date Of Signature

Signature of Chairman (with date), Oral Examination Board

Acknowledgements

I am very thankful to **Dr Yuvraj Kumar Madhukar** for trusting me and providing me with the opportunity to perform this research work under his valuable supervision. He has always shown me the correct way to me for solving problems related to the research work. He motivated me and gave his great ideas with important key points to me for understanding the depth of the subject. I am thankful to him, also for building confidence in me to successfully complete this research work. His suggestions and comments helped me to modify the research work in a positive direction. I take my deep sense of respect and gratitude for him for his guidance and lessons. I feel the privilege to be one of his students.

My gratitude is also extended to my PSpC members **Dr Hemant Borkar** and **Dr Kazi Sabiruddin** for their valuable guidance, suggestions, and support in this research work.

. I express my sincere gratitude to my Ph.D. Scholar Mr Anas Ullah Khan and B. Tech students Shivam Sarle and Dil Parmar for their initial technical assistance to my project.

. I would also like to express my thanks to Mr Anand Petare, DGM, Central Workshop, and all the staff of Central Workshop, IIT Indore,

The Discipline of Mechanical Engineering, IIT Indore, is gratefully acknowledged for giving me an opportunity to carry out my M. Tech and needed thesis research work. A heartfelt thanks to my entire M. Tech 2020 Batch.

Last, but not least, I would like to thank almighty GOD and all members of my family. They always give me strength, motivation, confidence, and love to successfully perform all tasks of my life.

Prabhat Mishra

**Dedicated to My Family & all the
Teachers**

Abstract

Additive manufacturing (AM) is defined as “a process of joining materials, usually layer upon layer, to make objects from 3D model data.” According to ASTM- “AM is the opposite of subtractive methodologies.” [1]. It is a rapidly growing technology that is showing great potential at lowering the production costs by reduction of material wastage and reduction of the time to manufacture. Additionally, it gives more freehand to the designers. [2]. Metal AM has a commonplace in various sectors i.e., aerospace industries, automotive industries, energy generation industries, and medical industries. It is expected that these industries will capture more than 80% of the additive manufacturing market by 2025 [3].

Additive manufacturing (WAAM) is one of the various variants of the DED technique, which is a modified process of welding processes such as gas metal arc welding (GMAW), gas tungsten arc welding (GTAW), plasma arc welding (PAW) [4]. WAAM has more to promise than previous AM technologies since it advances due to a better effective metal deposition rate, lower energy consumption, improved energy efficiency, a wider range of accessible materials, and lower equipment costs due to no abrasion of machine and tool parts. [5]. In our studies, we have focused on implementing an innovative and efficient WAAM deposition method to fabricate stainless steel specimens using 2 wires to feed simultaneously (double-wire feed) [6] for deposition and Wire arc additive manufacturing process (DWF-WAAM) and try to make bead parameters more uniform by controlling the deposition parameter. Various characteristics exhibited by the DWF WAAM process will be studied and analysed i.e., the melt pool parameters and bead appearance along with bead parameter of the test components will be investigated. It was expected that the DWF-WAAM method can be applied for high efficiency and high deposition rate applications because the temperature and power distribution of arc between electrode and melt pool is bell-shaped and the wire that is fed covers a very less area of arc zone. So, a substantial amount of energy goes to the melt pool which can be utilized for second wire deposition [6]. Along with it, we have tried to make the bead parameters more uniform using some modifications in the deposition parameters.

Contents

LIST OF FIGURES	ix
LIST OF TABLES	xii
NOMENCLATURE.....	xiii
ACRONYMS	xiv
Chapter 1: Introduction	1
1.1 Additive Manufacturing.....	1
1.1.1 Additive Manufacturing.....	1
1.1.2 Industries and applications of additive manufacturing	3
1.2 Wire Arc Additive Manufacturing.....	4
1.2.1 Wire Arc Additive Manufacturing.....	4
1.2.2 Advantages of WAAM	6
1.3 Arc temperature and pressure distribution	7
1.3.1 Analysis of the distribution of arc pressure	7
1.3.2 Analysis of the distribution of arc temperature.....	9
1.4 Double Wire Feed WAAM process	10
1.5 organization of the thesis	10
Chapter 2: Review of past work and problem formulation.....	12
2.1 literature review	12
2.2 Objectives of the Present Research.....	14
2.3 Research Methodology	15
Chapter 3: Experimental details.....	17
3.1 Experimental setup.....	17
Chapter 4: Result and discussions.....	22
4.1 Observations for constant current SWF WAAM.....	22
4.1.1 Melt pool diagrams for different deposition conditions.....	22

4.1.2 Melt pool parameter variations with successive layers for different deposition conditions	24
4.1.3 Effect of deposition parameters on melt pool parameters.....	27
4.1.3 Deposited layer height variations with successive layers for different deposition conditions	32
4.1.4 Cross-sectional analysis for different deposition conditions	35
4.2 Observations for constant current DWF WAAM	37
4.2.1 Melt pool diagrams for different deposition conditions.....	37
4.2.2 Deposited layer height variations with successive layers for different deposition conditions for DWF WAAM.....	40
4.2.3 Comparison of deposition rate between SWF WAAM & DWF WAAM ..	41
4.3 Observations for decreasing current in succeeding layers for SWF WAAM	44
4.3.1 Melt pool diagrams for decreasing current in succeeding layers for SWF WAAM	44
4.3.2 Deposited layer height variations with successive layers for decreasing successive layer current deposition.....	45
Chapter 5: Conclusions and Future Scope	49
5.1 Conclusions	49
5.2 Future scope	50
References	51

LIST OF FIGURES

Figure Number & Figure Captions	Page No
Fig. 1.1 Application of Additive Manufacturing in various fields	4
Fig. 1.2 Deposition process schematic using WAAM	5
Fig. 1.3 Distribution of single arc under different currents.	8
Fig. 1.4 Distribution of single arc pressure with different arc lengths	8
Fig. 1.5 Temperature fields and velocity vectors in the arc and electrodes for 150 A arcs in argon	9
Fig. 1.6 Schematic diagram of DWF WAAM process	10
Fig. 3.1 pictorial representation of the experimental setup OF TIG	18
Fig.3.2 sample images of TIG deposited specimen	18
Fig. 3.3 DWF wire feeder alignment	19
Fig. 4.1 Melt pool diagram at 140 A current at 3 m/min WFS	23
Fig. 4.2 Melt pool diagram at 180 A current at 3 m/min WFS	23
Fig. 4.3 Melt pool diagram at 180 A current at 4 m/min WFS	23
Fig. 4.4 Melt pool diagram at 180 A current at 5 m/min WFS	24
Fig. 4.5 Melt pool parameter graph at 140 A current at 3 m/min WFS	25
Fig. 4.6 Melt pool parameter graph at 140 A current at 4 m/min WFS	25
Fig. 4.7 Melt pool parameter graph at 180 A current at 3 m/min WFS	26
Fig. 4.8 Melt pool parameter graph at 180 A current at 4 m/min WFS	26
Fig. 4.9 Melt pool parameter graph at 180 A current at 5 m/min WFS	27
Fig. 4.10 Melt pool length with current increased from 140 to 180A at 3 WFS	28

Fig. 4.11 Melt pool height with current increased from 140 to 180A at 3 WFS	28
Fig. 4.12 Melt pool length with current increased from 140 to 180A at 4 WFS	29
Fig. 4.13 Melt pool length with current increased from 140 to 180A at 4 WFS	29
Fig. 4.14 Melt pool length with WFS increased from 3 to 4 at 140A current	30
Fig. 4.15 Melt pool height with WFS increased from 3 to 4 at 140A current	31
Fig. 4.16 Melt pool length with WFS increased from 3 to 5 at 180A current	31
Fig. 4.17 Melt pool height with WFS increased from 3 to 5 at 180A current	32
Fig. 4.18 Variation of deposited layer height with successive layers at 140A & 3 WFS	33
Fig. 4.19 Effect of increasing WFS from 3 to 4 m/min at 140 A current on bead layer height	34
Fig. 4.20 Effect of increasing current from 140 to 180 A at 3 WFS on bead layer height	35
Fig. 4.21 Cross-section images at different deposition parameters at 200 mm/min travel speed	36
Fig. 4.22 Bar chart showing the Effect of current and WFS on bead cross-sectional parameters	36
Fig. 4.23 Melt pool images for DWF WAAM at 170 A current, a total of 3 WFS, and 200 mm/min deposition speed	38
Fig. 4.24 Sample images of DWF deposited specimen at a total of 4.8 WFS	38
Fig. 4.25 Melt pool size at 170 A and 3 WFS for SWF WAAM	39
Fig. 4.26 Melt pool size at 170 A and 3 WFS for DWF WAAM	39
Fig. 4.27 Layer height for deposition at 140A 4.8 WFS & 180A 8 WFS	41
Fig. 4.28 Deposition rate comparison for SWF &DWF at 140A current	43

Fig. 4.29 Deposition rate comparison for SWF & DWF at 180A current	43
Fig. 4.30 Melt pool diagram for decreasing current from 210A to 120A current at 4 m/min WFS	45
Fig. 4.31 Melt pool length and height variation for decreasing successive layer current at 4 WFS	45
Fig. 4.32 Deposited layer thickness variation for decreasing successive layer current	47
Fig. 4.33 Deposited layer height comparison between constant & decreasing successive layer current at 3 WFS	48
Fig. 4.34 Deposited layer height comparison between constant & decreasing successive layer current at 4 WFS	48

LIST OF TABLES

Table Number & Table Captions	Page No
Table 1 Chemical Composition of ER70S6	17
Table 2 TIG parameters for constant current SWF WAAM process	19
Table 3 TIG parameters for constant current DWF WAAM process	20
Table 4 TIG parameters for decreasing current in successive layers for SWF WAAM process	20
Table 5 Effect of current and WFS on bead cross-sectional parameters	36
Table 6 comparison of deposition between SWF WAAM and DWF WAAM	42
Table 7 Deposited layer thickness variation for decreasing successive layer current	46

NOMENCLATURE

I	Current
V	Voltage
w	Melt pool width
h	Melt pool height
l	Melt pool length
t	Bead height
T	Temperature
P	Arc pressure
d	Wire diameter
A	Ampere
H	Maximum specimen height
W	Maximum specimen width

ACRONYMS

AM	Additive Manufacturing
DED	Direct Energy Deposition
WAAM	Wire Arc Additive Manufacturing
GMAW	Gas Metal Arc Welding
GTAW	Gas Tungsten Arc Welding
TIG	Tungsten Inert Gas
MIG	Metal Inert Gas
SWF	Single Wire Feed
DWF	Double Wire Feed
WFS	Wire Feed Speed
PAM	Plasma Arc Additive Manufacturing
ND & IR	Neutral Density & Infra-Red
CNC	Computer Numerical Control
WF	Wire Feeder
CWF	Cold Wire Feeder
ROI	Region Of Interest
SOD	Stand-Off Distance

TS	Travel Speed
AC	Alternate Current
DC	Direct Current

Chapter 1: Introduction

1.1 Additive Manufacturing

1.1.1 Additive Manufacturing

The ASTM association defines additive manufacturing (AM) as “a process of joining materials to make objects from 3D model data, usually layer upon layer, as opposed to subtractive manufacturing methodologies” [7]. Much more additive manufacturing machines and methods are on their way to mainstream production lines. With the advent of new and better polymer and metal/alloy materials, as well as increased deposition speed and improved deposition precision and machine accuracy, Additive manufacturing has the ability to make parts and products with intricate features that traditional manufacturing procedures couldn't produce with ease.

Key elements of additive manufacturing

- Unparalleled Design Freedom-design for manufacturing
- Accurate, Reliable, and Repeatable Parts
- Print from the Cloud — Anywhere in the World
- Engineering-grade Durability with High-Strength Parts

It has not been that long since the quality of additive manufacturing has been improved to such a level that it has started showing its potential in industries as a viable method and proved to be a substitution for many traditional production technologies. With the advent of new and better polymer and metal/alloy materials, as well as increased deposition speed and improved deposition precision and machine accuracy, Additive manufacturing has the ability to make parts and products with

intricate features that traditional manufacturing procedures couldn't produce with ease. [8]. Additive manufacturing also processes various characteristics that provide it with the distinct ability to manufacture parts that cannot be manufactured by traditional manufacturing techniques or which could not easily have been manufactured via subtractive or other traditional manufacturing processes.

Various materials are used in additive manufacturing as Thermoplastic polymers (Acrylonitrile butadiene styrene (ABS), polylactic acid (PLA) and polycarbonate (PC)), metals, ceramics, and Biochemical (silicon, calcium phosphate, and zinc). although polymers are most commonly used and some additive techniques incline themselves towards the use of certain materials over others but with the advancement in the technology other materials have also started holding the substantial space in additive manufacturing production line up.

There are a lot of material deposition techniques which divide into 7 types-

- Powder Bed Fusion.
- Material extrusion.
- Vat photopolymerization.
- Direct Energy Deposition.
- Material jetting.
- Binder jetting.
- Laminated object manufacturing (LOM).

The types of additive manufacturing are categorized with their own characteristics, methods of deposition, the equipment used, and the type of power source for deposition. The type of additive manufacturing we are going to use in our project is Directed Energy Deposition (DED). DED is complex in nature of deposition due to its requirement of proper positioning for deposition and rigid structure to avoid variation in deposition having similar deposition conditions. The multiple axis arm will have an electrode mounted on it and will move as per the CNC

coding, producing an arc between electrode and substrate plate and depositing molten wire material on a specified path. The feed wire material is melted by a direct energy power source and will then solidify.

1.1.2 Industries and applications of additive manufacturing

Although additive manufacturing has not been able to show its full potential in production industries but new and innovative applications are continuously being explored and developed. From prototyping and tooling to directly utilized in part manufacturing in industries such as architectural, medical, dental, aerospace, automotive, furniture and jewellery, and many others [9]. The main fields which are using additive manufacturing extensively are as follows.

- **Lighter parts:** AM has a good hand at keeping the produced part light in weight and being able to manufacture complex design parts simultaneously.
- **Automotive:** Rapid prototyping is used in the automotive sector for part manufacture. Aluminium alloys, for example, are utilised to make exhaust and pump assembly parts.
- **Medical:** Medical and orthopaedic applications for AM are growing rapidly, especially with the improvement in the safety of medical devices built by AM, which are well checked and established. The sectors have also been introduced to additive manufacturing technology that creates custom, on-demand 3D printed surgical implants for patients.
- **Industrial Manufacturing:** With the realization of the potential for AM's design flexibility, design concepts that were considered unattainable early are now being considered again because additive

manufacturing has shown innovative and creative potential for designers.

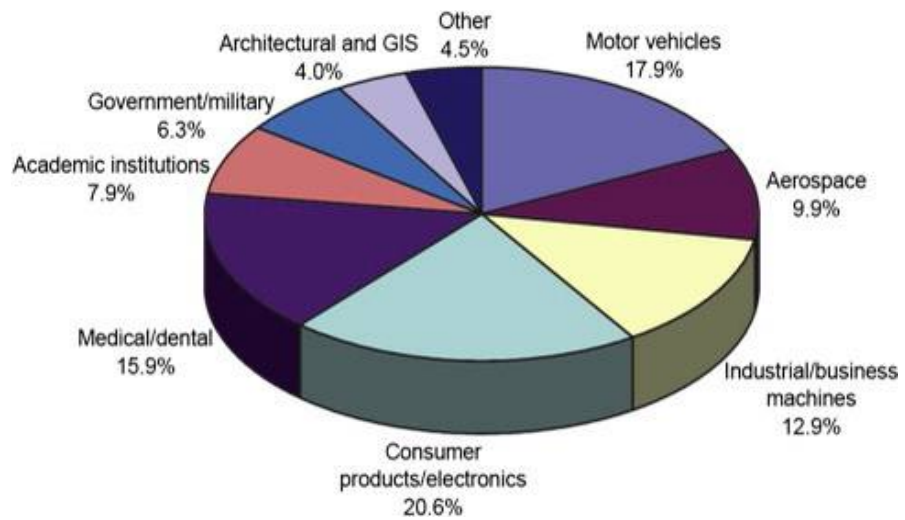


Fig. 1.1 Application of Additive Manufacturing in various fields

The newer systems and the broader range of materials being developed are increasing the effectiveness and adaptability of systems, improving productivity, printing resolution and precision, production volumes, and loading/unloading procedures. All these advancements will help in decreasing the costs of additive manufacturing compared to traditional manufacturing processes, ultimately pushing further industry adoption and expanding the range of useful applications.

1.2 Wire Arc Additive Manufacturing

1.2.1 Wire Arc Additive Manufacturing

The Direct Energy Deposition (DED) family of Additive Manufacturing methods includes Wire Arc Additive Manufacturing (WAAM). WAAM is defined as the “Process of depositing metal layers on top of each other until the required 3D shape is achieved.” It is a hybrid of two manufacturing techniques: gas metal arc welding

(GMAW) and additive manufacturing. Metal parts have been joined using the GMAW welding process, which uses an electric arc as a heating source., with or without additive material. In industries, 3d printing is referred to as additive manufacturing. A welding robot is coupled with a power supply in the WAAM process for generating continuous

arc, for manufacturing of parts. An electrode is attached to the robot which generates a continuous arc between electrode and substrate plate and It's used to melt wire feedstock to make the 3D item.

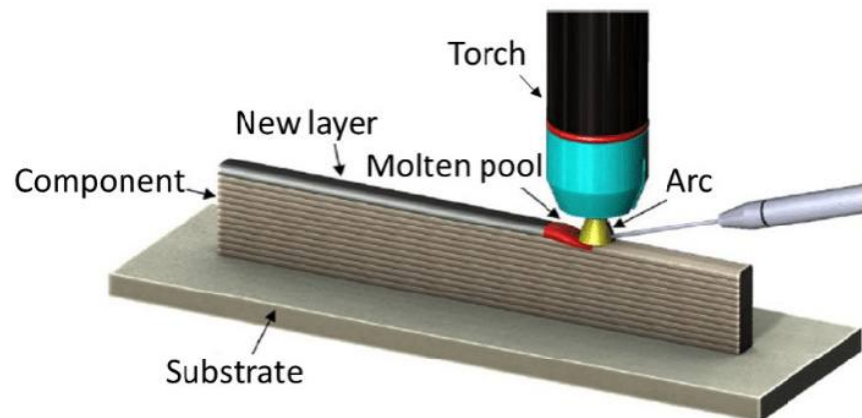


Fig. 1.2 Deposition process schematic using WAAM

Wire arc additive manufacturing (WAAM) is nowadays known as directed energy deposition-arc (DED-arc). It is mainly incorporated into manufacturing industries for increasing manufacturing efficiency so that produced parts can have better qualities without increasing the production cost. It can create complex shapes without the use of specific tools, resulting in cost and time savings without sacrificing quality. Local setup installation will reduce inventory requirements and allow for the fulfilment of particular and urgent requests.

A typical AM system is made up of a movement supplier, a heat source, and feedstock.

1.2.2 Advantages of WAAM

- **Size freedom:** The limit of the size of the deposited part mainly depends on the reach of the deposition head that is used which can be modified with robot tracks.
- **Additional design freedom:** WAAM method allow facilitates the manufacturing of relatively complex design geometries which infers that topological optimization is more accessible than traditional methods.
- **Low initial cost:** Compared to some other DED systems WAAM deposition can be done at a reduced cost.
- **Higher deposition rate:** Due to its very basic yet effective design of deposition it can deposit the material at a higher rate compared to other AM processes.
- **Range of available material:** WAAM uses feed wires for depositing materials. As per the requirement of the application, various choices of materials can be converted into wire form for ease of deposition.
- **Combined manufacturing:** For imparting the special features or for ease of production WAAM can be simultaneously used with other production methods to build any part.
- **Combined materials:** layered manufacturing and double wire feed manufacturing can be used to make functionally graded material in which a range of materials can be combined to deposit the part.
- **Waste reduction:** Material is only deposited where needed, which leads to a waste reduction thus it has great potential for parts that require material to be removed out of the main part in traditional production method and/or for parts that are built by expensive materials. Topological optimization can further improve the efficiency of deposition.
- **Mechanical properties:** Processes like preheating, after rolling post-heating can improve the mechanical properties of WAAM-built products compared to traditionally manufactured products.

Process parameters affecting the WAAM process

WAAM process depends on several process parameters such as wire feed rate, travel speed, current, shielding gas flow rate, arc voltage, working distance, deposition strategy, heat input, etc. The properties of bead profile and deposition parameters such as bead depth, bead width, roughness, wetting angle, and bead geometry complete melting of deposition material directly or indirectly depend on these parameters [10]. These deposited parameters mainly depend on heat input which depends on current and travel speed. Increasing current and decreasing travel speed causes an increase in heat input. All these parameters should be considered for the successful deposition using the WAAM process.

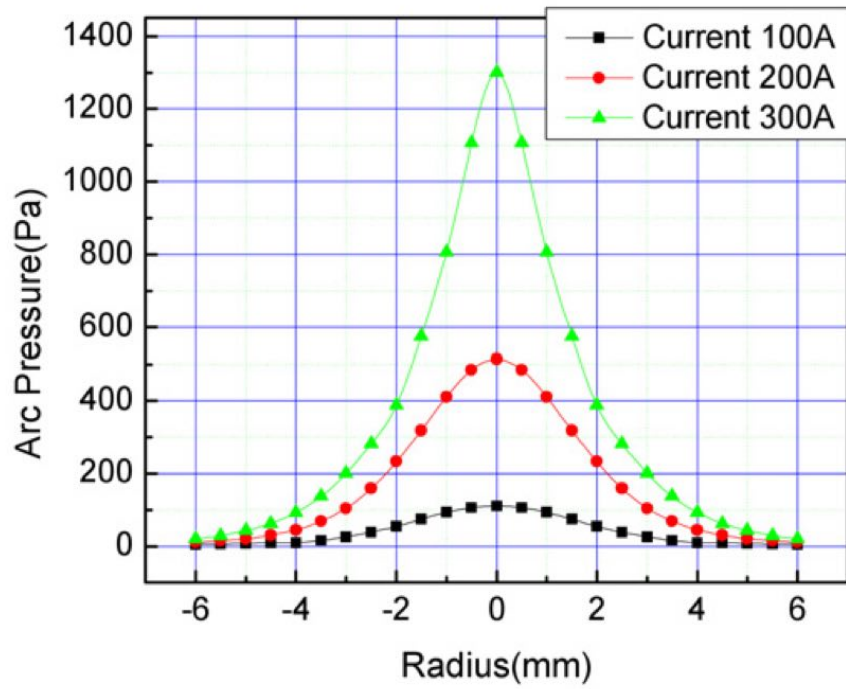
1.3 Arc temperature and pressure distribution

1.3.1 Analysis of the distribution of arc pressure

Arc pressure is the force that acts on the anode due to the generation of electromagnetic fields in the arc zone. Arc pressure is an important physical characteristic of the arc, and it has a direct effect on the deposited bead appearance and the metal deposition rate as it facilitates the molten drop to get deposited effectively the arc pressure drives the molten metal to the back of the molten pool during the deposition process, allowing the arc to directly heat the material beneath it. The molten pool, however, will be burned through if the arc pressure exceeds the allowable limit. Such faults as undercut, pit and splatter will emerge in a high-speed deposition process, so arc pressure should be kept within a certain range. [11].

The maximum value of the arc pressure increases current goes above

and arc length falls below the permissible range, and the distribution



shapes also change with it.

Fig. 1.3 Distribution of single arc under different currents.

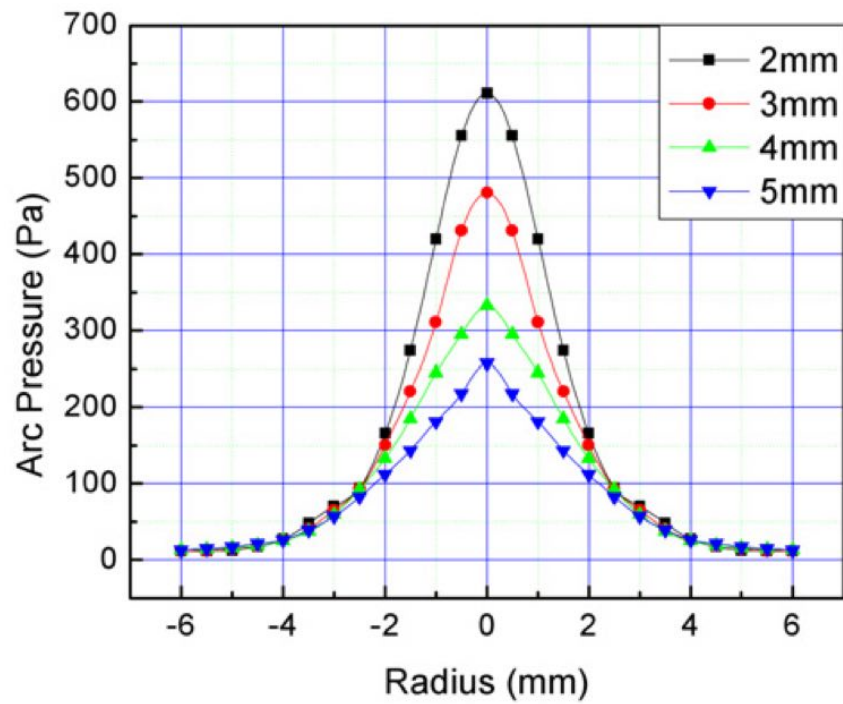


Fig. 1.4 Distribution of single arc pressure with different arc lengths

1.3.2 Analysis of the distribution of arc temperature

The temperature distribution in the arc between electrode and melt pool is bell-shaped. Its distribution area should be wide enough for introducing wire and also the temperature should be sufficiently high that it could melt the depositing wire. The distribution of temperature changes with the shielding gas used, for argon gas the arc distribution zone is substantially larger than the deposition wire material and also sufficient temperature to melt the depositing wire, it has a low anode (workpiece) temperature which is beneficial as it will avoid remelting of the deposited material thus giving good tolerance and also it has low gas flow velocity which is also beneficial as it tends to help in cutting not depositing [10].

The temperature interval is 2000 K in the arc, 200 K in the cathode, and 100 K in the anode.

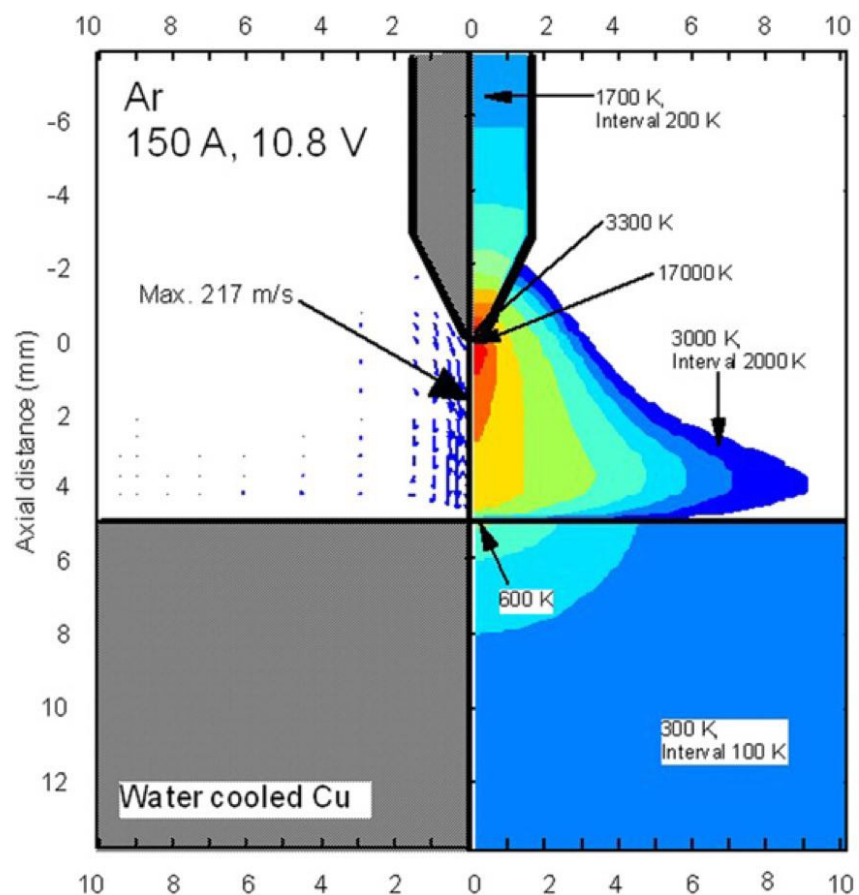


Fig. 1.5 Temperature fields and velocity vectors in the arc and electrodes for 150 A arcs in argon

1.4 Double Wire Feed WAAM process

Many researchers have employed arc-based additive manufacturing with multiple wires to produce hybrid deposition of dissimilar metals. Shen et al. (2015) used a GTAW-based deposition technique to produce steel components rich in Fe-Al intermetallic compounds [6]. Almost all of these researchers have used the DWF approach to create functionally graded materials or composite materials, with little emphasis on increasing deposition rate without sacrificing quality.

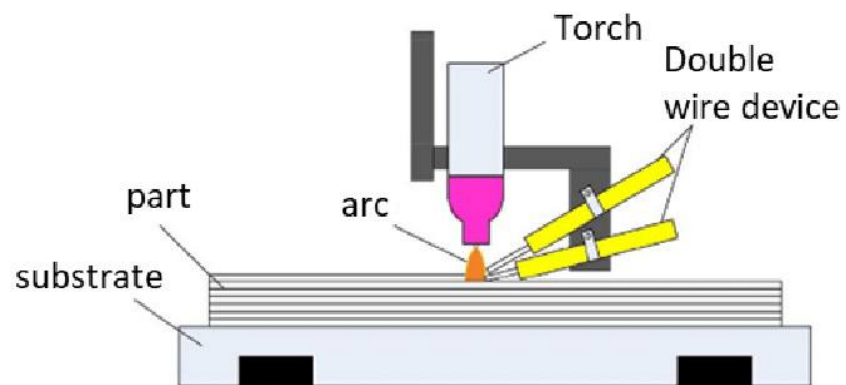


Fig. 1.6 Schematic diagram of DWF WAAM process

1.5 organization of the thesis

Chapter 2 presents a detailed literature review on the past work reported in the relevant field of wire arc additive manufacturing, tungsten inert gas welding, and its automation, monitoring of WAAM, parameters of the objectives of the research, and the research methodology used in the present work Also methods of controlling of the melt pool and bead

Chapter 3 includes the experimental setup of the SWF and DWF TIG-based WAAM process and various parameters at which the experiments have been performed.

Chapter 4 includes the measurement of the melt pool and bead parameters at various parameters and their analysis for SWF, DWF, and decreasing successive layer current.

Chapter 5 Highlights the conclusions of the present work and marks the scope for future work based on the limitations of the present work.

Chapter 2: Review of past work and problem formulation

2.1 literature review

This chapter covers the crux of the literature assessment, including limitations, on previous work on the subject of wire arc-based additive manufacturing, control parameters of TIG based processes, heat and temperature distribution in the arc, effect of deposition parameters on the melt pool parameters, the identified research gaps, the research objectives defined to bridge the identified research gaps and research methodology used in the present work.

Yildiz et al. used the WAAM system to fabricate High-strength low-alloy steel specimens using various deposition strategies and process parameters. Wire feed speed (WFS) and WFS/TS (travel speed) ratio were selected as key process parameters and their effect on mechanical properties and characteristic bead dimensions were investigated. WFS/TS ratio was found to be the most crucial process parameter for controlling heat input [12]. In the study, it was found that the heat input linearly correlated with the characteristic bead dimensions i.e., bead height, width, penetration area, penetration, and reinforcement area.

Sun et al. in their analysis employed a coaxial imaging system for determining the melt pool cross-sectional geometry [13]. They used 5 image processing steps to get the desired image which could give the melt pool parameters needed for the analysis, namely the original image, gamma-corrected image, noise removed image, contrast-enhanced image, and at last edge extraction of the melt pool. Their study provides relatively easy and less cumbersome but still provides the sufficiently accurate results of melt pool parameters.

Soylemez et al. proposed an analytically-guided approach to maintain the constant melt pool cross-sectional area [14]. Modelling results show

how a constant power(P)/travel velocity(V) ratio can control the melt pool area and shape L (melt pool length)/d (area average diameter) and also shows how a $P/V = \text{constant}$ proposal for maintaining melt pool dimensions can fetch poor results, especially in case of small-scale processes.

Dinovitzer et al. analysed the effect of varying the process parameters in TIG-based WAAM specimen using the Hastelloy as deposition material wire and concluded that with wire feed rate Bead height increases linearly [15].

Travel speed and current have the inverse effect on the heat input and therefore show similarity in the trends but in opposite directions. Their study also shows Increase in travel speed or a decrease in current causes melt through depth to decrease along with an increase in roughness. Bead width shows a decreasing trend with travel speed and the Melt through depth shows a decreasing trend with travel speed. Their studies help in controlling the bead parameters while depositing in the WAAM process.

Montevecchi et al. proposed a WAAM modelling strategy that was based on a heat source model that considers the actual power distribution between electrode and substrate material [16]. The effectiveness of the proposed model was proved by an experimental validation with the help of a comparison between the measured distortions for the WAAM tests case and the simulated model. They have proposed a double ellipsoid heat source model and prescribed Gaussian distribution of heat generation per unit volume.

Leng et al. described the distribution of arc pressure while depositing with the TIG method and also analysed the effect of welding current, electrode distance, and arc length on arc pressure [11]. Since the arc pressure is an integral characteristic of arc and it has a substantial effect on the bead appearance and deposition rate. The peak arc pressure increases with arc current and decreases with arc distance. Control of arc pressure is essential as excessive arc pressure will burn through the

molten pool as it pushes the molten material to the rear of the molten pool.

Murphy et al. Reviewed the effect of thermophysical properties of shielding gas on the TIG arc especially those which affect the weld pool [7]. Their studies suggested that weld pool depth can be increased by using shielding gas of high thermal conductivity and specific heat. Higher electrical conductivity of metal vapour causes low heat flux thus a shallower weld pool. Their studies guided us that argon is a good option as shielding gas for our purpose as it has sufficient temperature to melt the deposition wire and also enough distribution zone of temperature that a second wire could be introduced easily along with less heat at substrate material ensuring there is no remelting of the already deposited material.

Feng et al. proposed an innovative process to increase the deposition rate using stainless steel as deposition material using a double wire feed (DWF) set up in the Plasma arc additive manufacturing process and they got succeeded in their efforts [6]. Also, along with the increased deposition rate for DWF PAM the mechanical properties improved with respect to the single wire feed PAM process. This increase in deposition rate indicated that deposition rate could also improve with a double wire feed setup when applied in Wire arc additive manufacturing (WAAM).

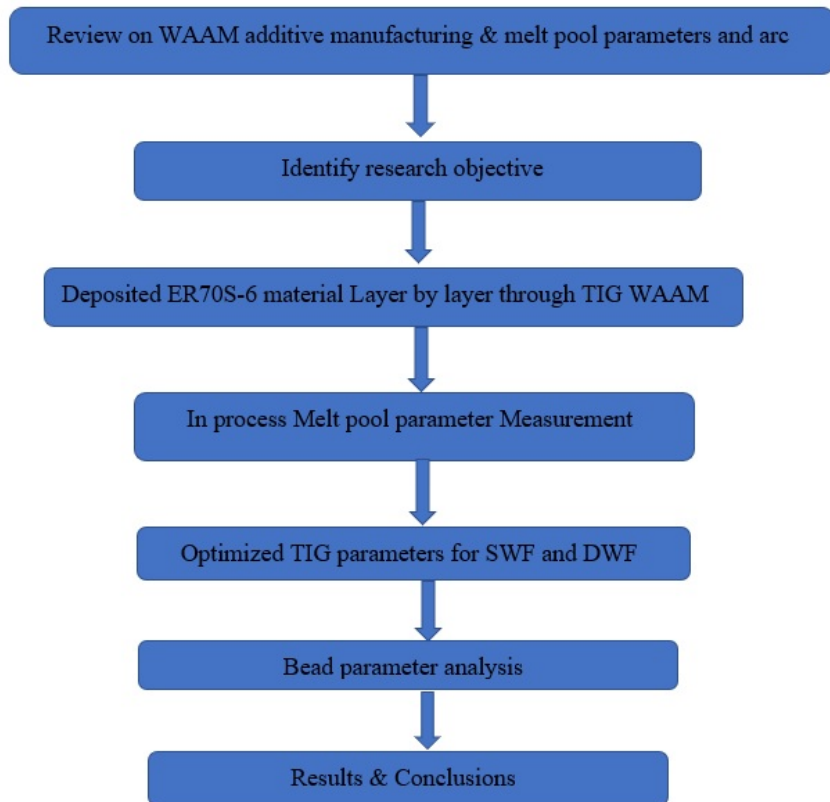
2.2 Objectives of the Present Research

- Observing if the increase in wire deposition rate takes place without increasing the power input for DWF WAAM.
- Compare the melt pool parameters changes for DWF-WAAM with respect to the SWF-WAAM process.

- Optimization of parameters for efficient deposition
Optimization: GTAW-based WAAM process shall be employed for the execution of the objectives. ER70S-6 wire of a diameter of 0.6 mm will be used as deposition material.
- Employing methods to make bead parameters uniform by controlling deposition parameters.
- In Situ monitoring of WAAM melt pool: a high speed (500 fps) colour camera will be employed for the purpose. different ND & IR filters of different optical densities will be employed to prevent the arc light from interfering with the melt pool image.
- Control of melt pool size during the WAAM process: arc current, wire feed rate, and deposition speed would be optimized.

2.3 Research Methodology

After reviewing the literature, we have tried to increase the deposition rate by using TIG based WAAM process and also to make the bead parameter more uniform by controlling the deposition parameters. First, we deposited the linear layered specimen using the SWF WAAM process and observed the maximum WFS that could be achieved with complete melting, and then we did the same process for DWF WAAM to find the maximum achievable WFS with complete melting. Then the parameters of weld pool and bead have been analysed and we observed if the deposition rate was increased for the DWF WAAM and bead parameters variation with layers. Finally, attempts have been made to make the bead parameter more uniform by decreasing current in successive layers so that melt pool parameters could be controlled which could control the bead parameters and make the bead parameters more uniform. The methodology has been shown in the flow diagram below.



Chapter 3: Experimental details

3.1 Experimental setup

The in-house developed WAAM setup was used to perform the experiments. The SNPS power source mode was used for the deposition of WAAM beads. The optimized deposition parameters were used and kept constant throughout the experiments i.e., 200 mm/min deposition speed. A low alloy steel wire ER70S6 of 0.6 mm diameter was used as deposition material (wire electrode). Table 1 shows the chemical composition of ER70S6.

Table 1

Chemical Composition of ER70S6:

C	Si	Mn	P	S	Ni	Ti+Zr	Cr	M
o	V	Cu	Al					
0.07	0.92	1.55	0.012	0.012	0.03	0.019	0.04	0.01
	0.01	0.24	0.009					

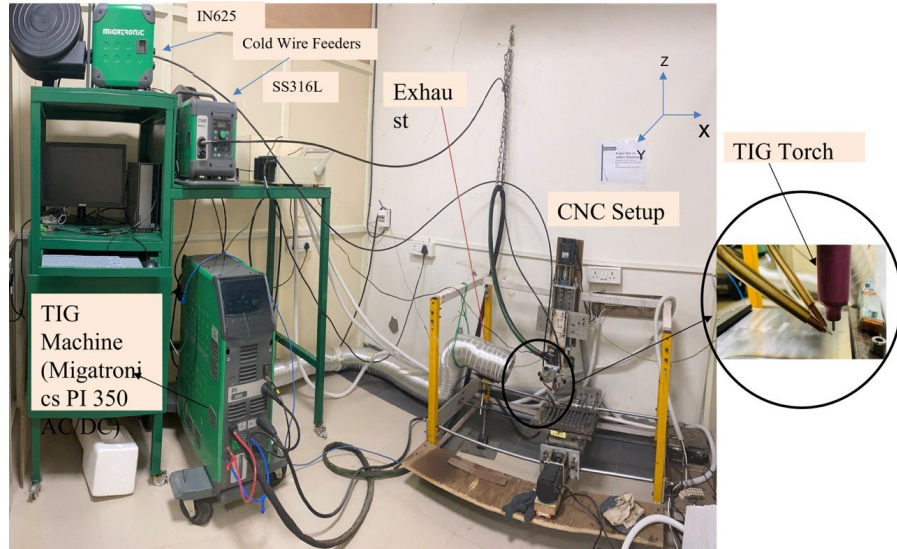


Fig. 3.1 pictorial representation of the experimental setup OF TIG

The deposition (TIG) torch was mounted on the Z-axis of the CNC workstation to facilitate the process. The work plate was mounted on a



Fig.3.2 sample images of TIG deposited specimen

movable fixture that could provide XY movements. The movements were controlled and carried out by a Mach3 CNC controller. A substrate plate of AISI 1020 low carbon steel of 5 mm thickness was used for the deposition purpose. Argon was used as a shielding gas at a constant flow rate of 10 l/min. A tungsten electrode (2% thoriated) of 2.4 mm diameter was utilized at a constant standoff distance of 4 mm.

For the single wire feed constant current WAAM process WFS kept constant at 200 mm/min and deposition was done at 140 and 180A

current, 3 levels of WFS has used 3,4 and 5 m/min, and melt pool parameters, bead parameters, and cross-section parameters were observed for analysis. Single line layered deposition of 70 mm length was carried out for the study and a total of 10 layers have been deposited.

Table 2

TIG parameters for constant current SWF WAAM process

Current (A)	140	140	180	180	180
WFS (m/min)	3	4	3	4	5

For DWF constant current of 140A and 180A was used at a travel speed of 200 mm/min, Total WFS was started from 3 m/min and increased up to 4.8 m/min for 140A current and 8m/min for 180 A current. The electrode vertex angle was kept at 45° for both the wire feeders. Melt pool parameters and bead parameters were carried out for analysis and Single line layered deposition of 70 mm length was carried out for the study and a total of 10 layers have been deposited.

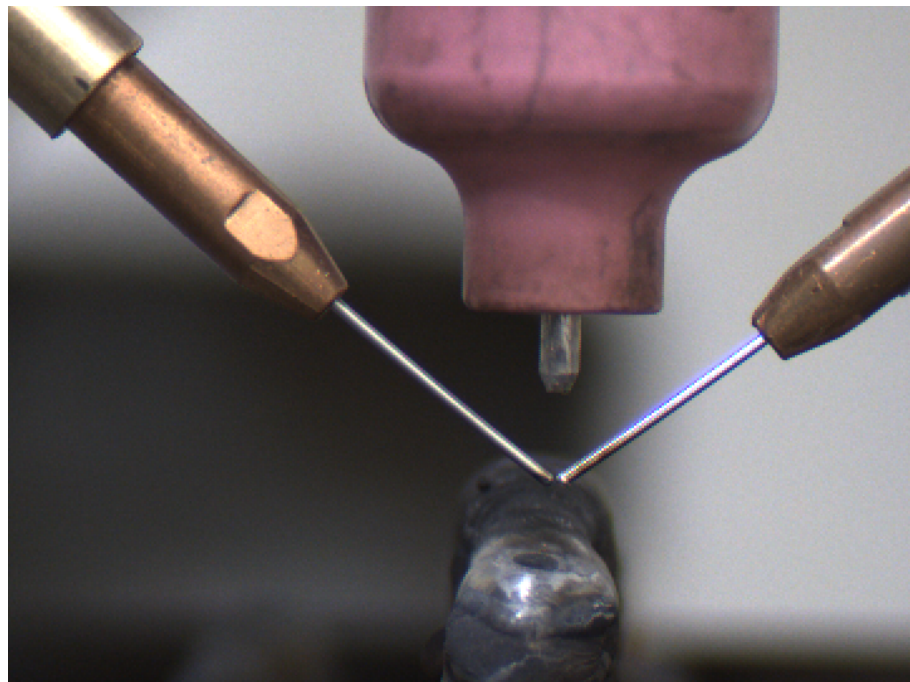


Fig. 3.3 DWF wire feeder alignment

Table 3**TIG parameters for constant current DWF WAAM process**

Current (A)	140	140	140	180	180	180
WFS (m/min)	3	4	4.8	4	5	8

Table 4**TIG parameters for decreasing current in successive layers for SWF WAAM process**

Layers	1	2	3	4	5	6	7	8	9	10
Current (A) Ex. 1, 3WFS	180	175	170	165	160	150	140	130	120	110
Current (A) Ex. 2, 4WFS	210	200	190	180	170	160	150	140	130	120

For controlling the bead deposition parameters deposition was carried out at decreasing current in successive layers, travel speed kept constant at 200 mm/min and 2 experiments were carried out at decreasing current in which current decreased from 180 to 110 in one experiment and 210 to 120 in another experiment. Melt pool parameters and bead parameters were carried out for analysis and Single line layered deposition of 70 mm length was carried out for the study and a total of 10 layers have been deposited.

For the analysis purpose of the melt pool video of the melt pool which was taken at 500 fps was analysed, the video was converted to images, and an average of melt pool parameters were taken for studies then image processing was done in ImageJ software so that contrast could be enhanced and melt pool could become more observable finally the image was converted to the 8-bit grey image so that edge detection could be used to identify melt pool zone. The electrode diameter of 2.4 mm which was visible in the videos was taken as a reference for measuring the melt pool parameters. Since the video was taken from the side view thus only melt pool length and melt pool height could be observed but not melt pool width so the results are as per the available melt pool parameters only.

For analysis of cross-section also image J was used and substrate plate thickness of 5 mm was taken as reference for measuring the cross-sectional and bead parameters and the edge detection ROI method was used for measuring the cross-sectional area of the deposited bead.

Chapter 4: Result and discussions

4.1 Observations for constant current SWF WAAM

4.1.1 Melt pool diagrams for different deposition conditions

At constant current SWF WAAM deposition when travel speed was kept constant and linear layered deposition was done then it was observed that melt pool parameters i.e., melt pool length and melt pool height, have shown an increasing trend with successive layers. The deposition was carried out at 2 values of constant current 140A and 180 A respectively. For 140A current at 3 WFS melt pool length increased from 5.518 at layer 1 to 11.211 at layer 10 and a similar increasing trend was observed for other depositions also at different deposition parameters. Fig 4.1, 4.2, 4.3 & 4.4 show the melt pool diagram with successive layers for different deposition parameters and the melt pool can be clearly observed from these images which show an increasing melt pool parameter trend.

The highest WFS at which wire can be deposited was between 3 to 4 m/min (take 3.5) for 140 A current at 200mm/min travel speed, at 4 m/min the deposition was not continuous and also not complete melting of wire was taking place at 4 m/min.

The maximum WFS was 5 m/min for 180 A at 200 mm/min travel speed. There was a limit in the WFS for the wire feeder of 5 m/min thus we could not increase the WFS more than 5 m/min but it was cross-checked that at 170 A current it was not able to deposit the wire at 5

m/min but at 180 A current deposition took place effectively, which ensures the maximum WFR was 5 m/min for SWF WAAM at 180 A current.

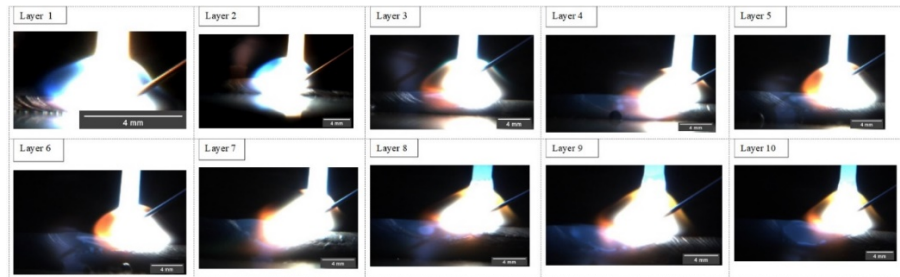


Fig. 4.1 Melt pool diagram at 140 A current at 3 m/min WFS

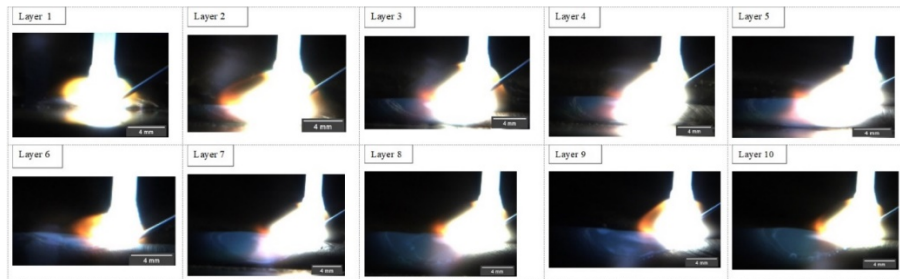


Fig. 4.2 Melt pool diagram at 180 A current at 3 m/min WFS

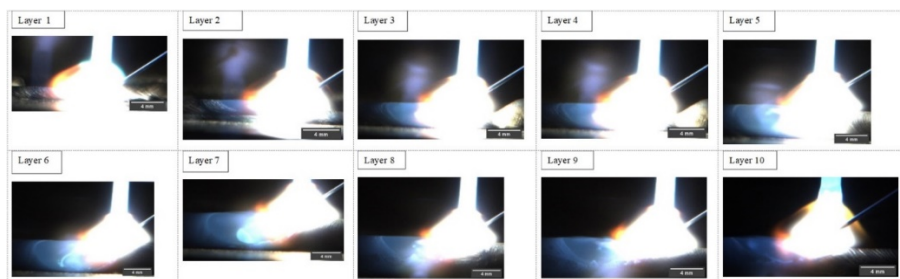


Fig. 4.3 Melt pool diagram at 180 A current at 4 m/min WFS



Fig. 4.4 Melt pool diagram at 180 A current at 5 m/min WFS

4.1.2 Melt pool parameter variations with successive layers for different deposition conditions

When the graph has been plotted for constant current SWF WAAM process then the melt pool length and melt pool height show an increasing trend with successive layers which can be easily observed with the graph. Since at initial layers the layer is deposited on the substrate plate or close to it thus the thermal conductive resistance is very less the heat loss rate is very high thus the majority of the heat gets lost through the substrate plate thus melt pool size is less initially but as the number of layers is increased then the distance of deposited layer with the substrate plate increases thus thermal conductive resistance gets increased each layer thus heat dissipation rate through conduction decreases with succeeding layers causing more heat to get accumulated in the melt pool zone itself thus melt pool size increases with successive layers, but in the latter, most layers the effect of increasing thermal conductive resistance gets stabilized thus very less increment in melt pool parameter can be seen in the lattermost layers. With the increase in the number of layers convective and radiative heat resistance gets decreased but the conductive heat resistance dominates over these 2 heat resistances thus there is not much effect of it in the initial deposition stages. Figures 4.5, 4.6, 4.7, 4.8 & 4.9 show the increasing trend of melt pool with successive layers for different current and wire feed rates.

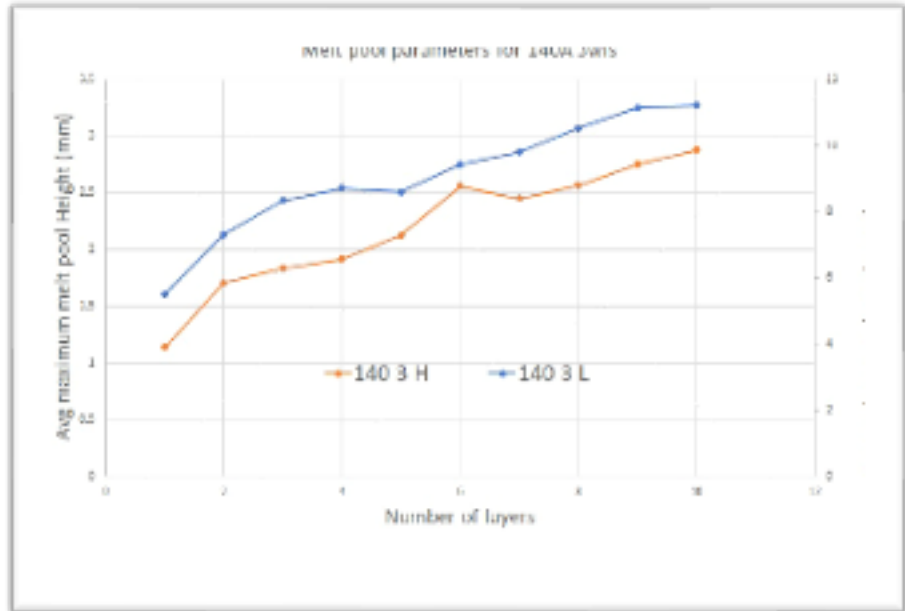


Fig. 4.5 Melt pool parameter graph at 140 A current at 3 m/min WFS

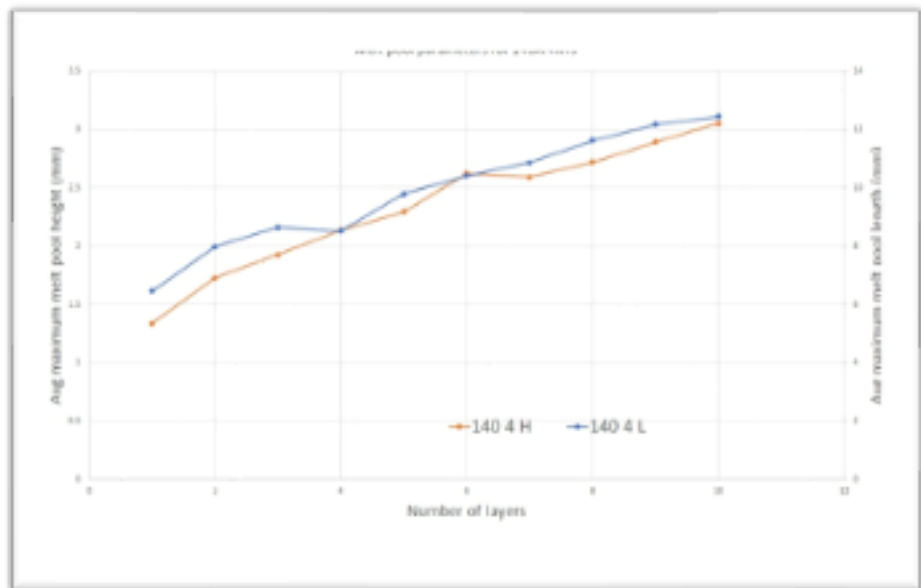


Fig. 4.6 Melt pool parameter graph at 140 A current at 4 m/min WFS

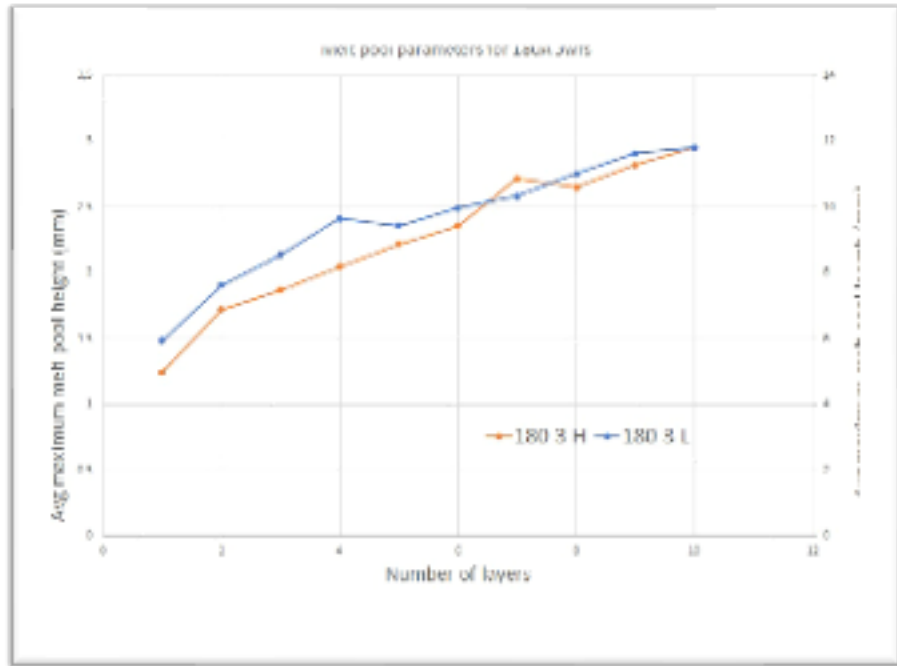


Fig. 4.7 Melt pool parameter graph at 180 A current at 3 m/min WFS

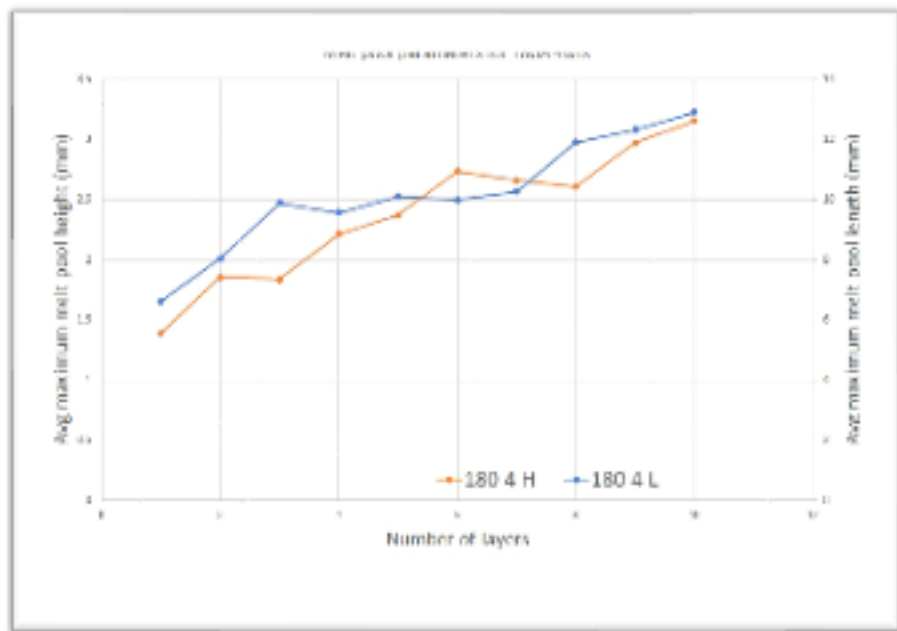


Fig. 4.8 Melt pool parameter graph at 180 A current at 4 m/min WFS

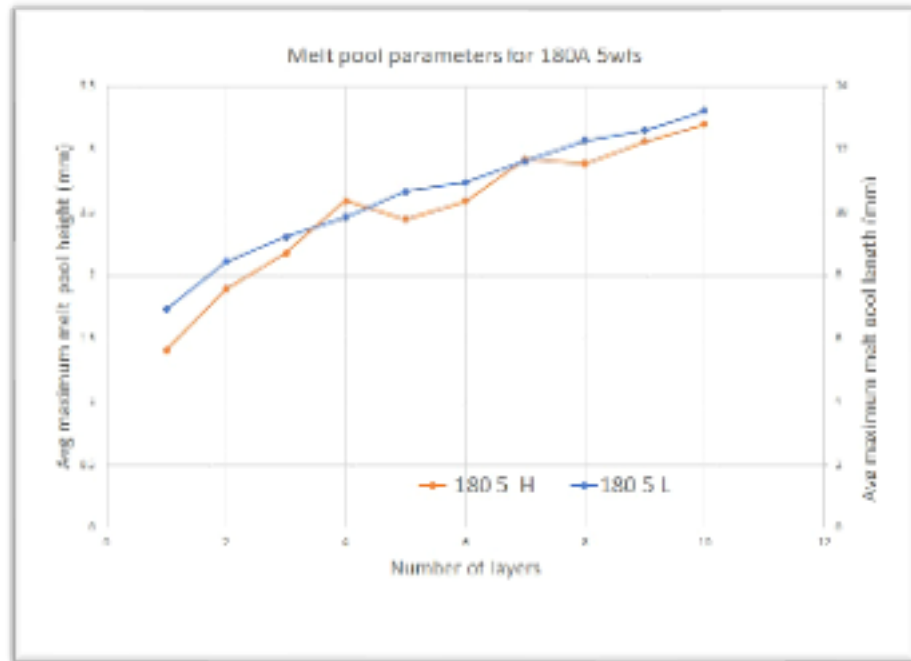


Fig. 4.9 Melt pool parameter graph at 180 A current at 5 m/min WFS

4.1.3 Effect of deposition parameters on melt pool parameters

With the increase in input heat, the melt pool parameter increases because more heat is available to melt the wire, and also more heat is available after melting the deposition wire. Also, with the increase in WFS and keeping all other parameters unchanged the melt pool parameters increase because more material gets melted and deposited per unit length.

4.1.3.1 Effect of increasing current on melt pool parameters

It can be observed from the graphs that with an increase in current keeping the other parameters unchanged, the melt pool length and height show an increasing trend. Fig 4.10, 4.11, 4.12 & 4.13 are the graphs showing the effect of changing the current on the melt pool length and melt pool height.

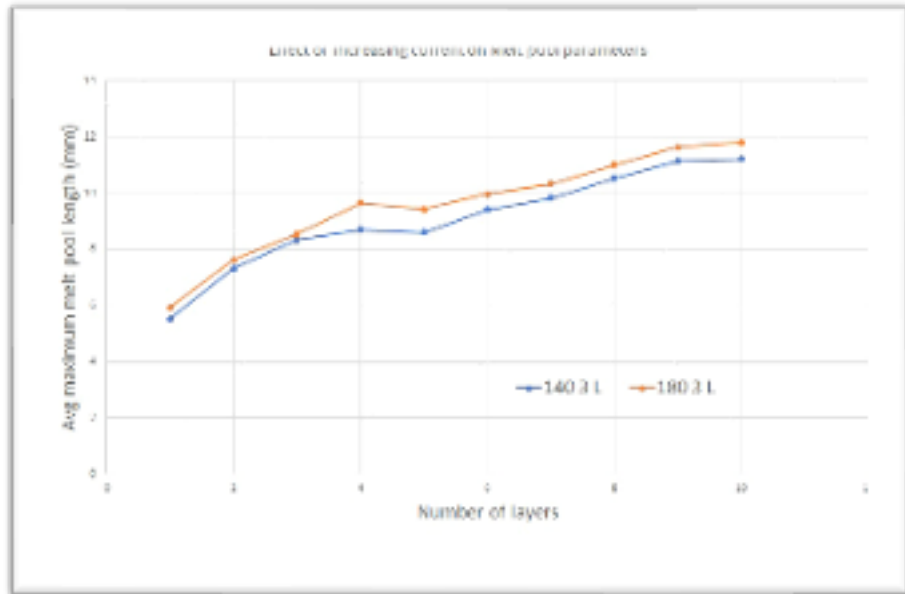


Fig. 4.10 Melt pool length with current increased from 140 to 180A at 3 WFS

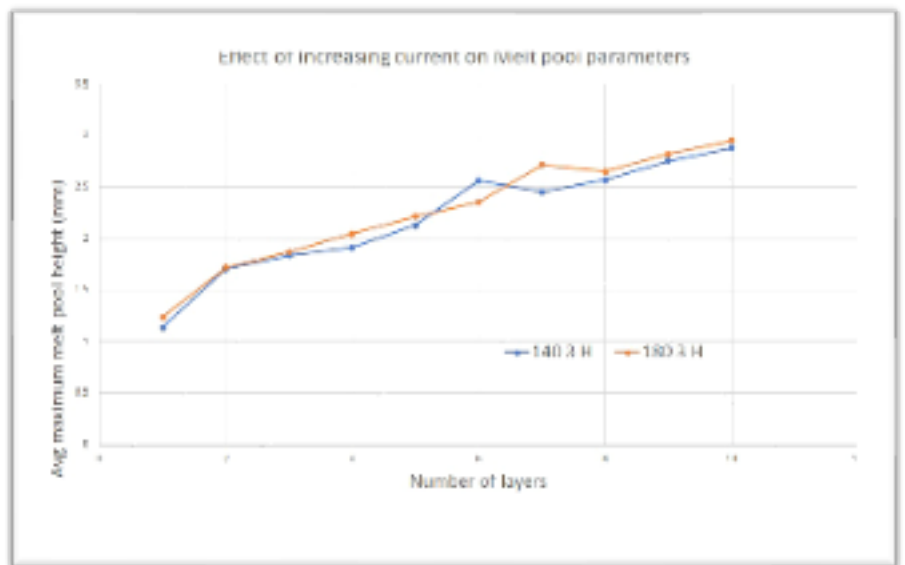


Fig. 4.11 Melt pool height with current increased from 140 to 180A at 3 WFS

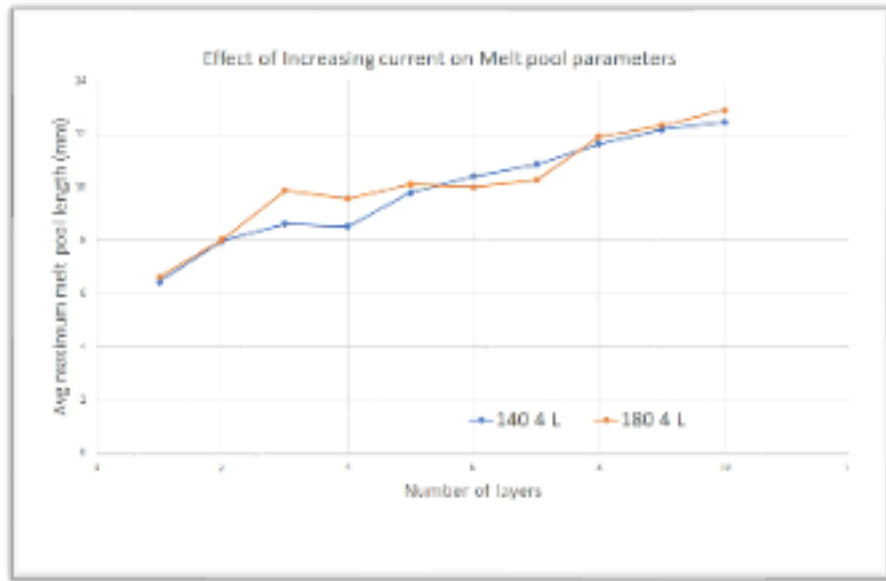


Fig. 4.12 Melt pool length with current increased from 140 to 180A at 4 WFS

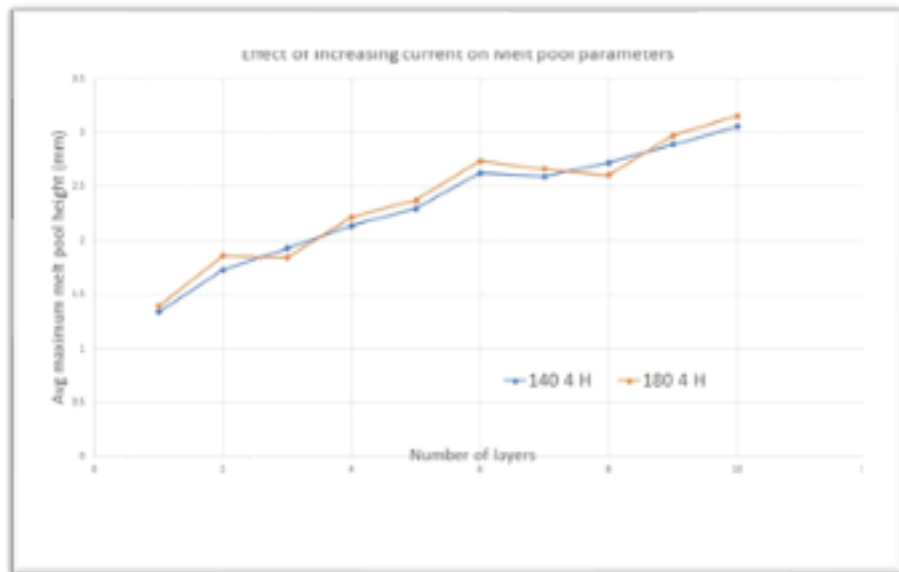


Fig. 4.13 Melt pool length with current increased from 140 to 180A at 4 WFS

4.1.3.2 Effect of increasing WFS on melt pool parameters

It can be observed from the graphs that with an increase in WFS keeping the other parameters unchanged, the melt pool length and height show an increasing trend. Fig 4.14, 4.15, 4.16 & 4.17 are the graphs showing the effect of changing the WFS on the melt pool length and melt pool height.

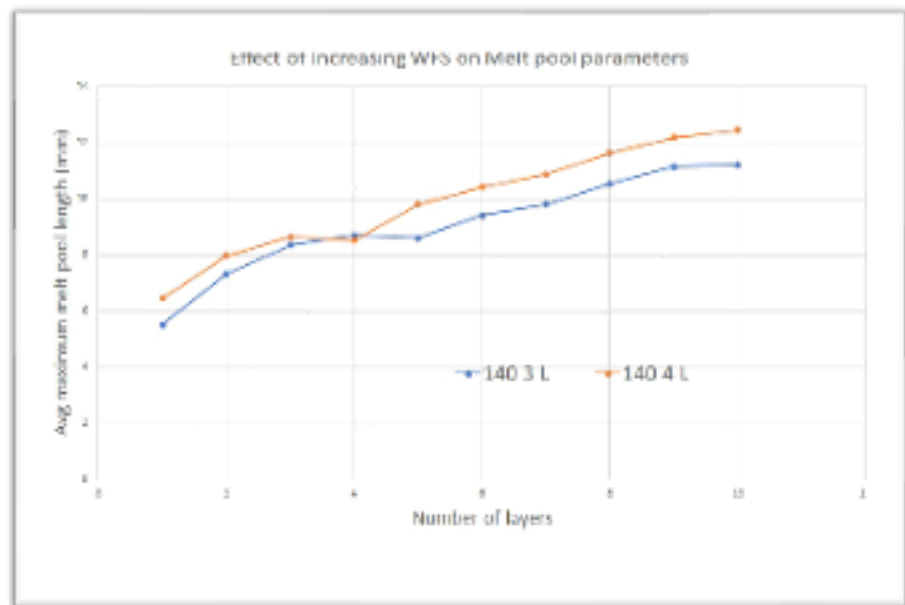


Fig. 4.14 Melt pool length with WFS increased from 3 to 4 at 140A current

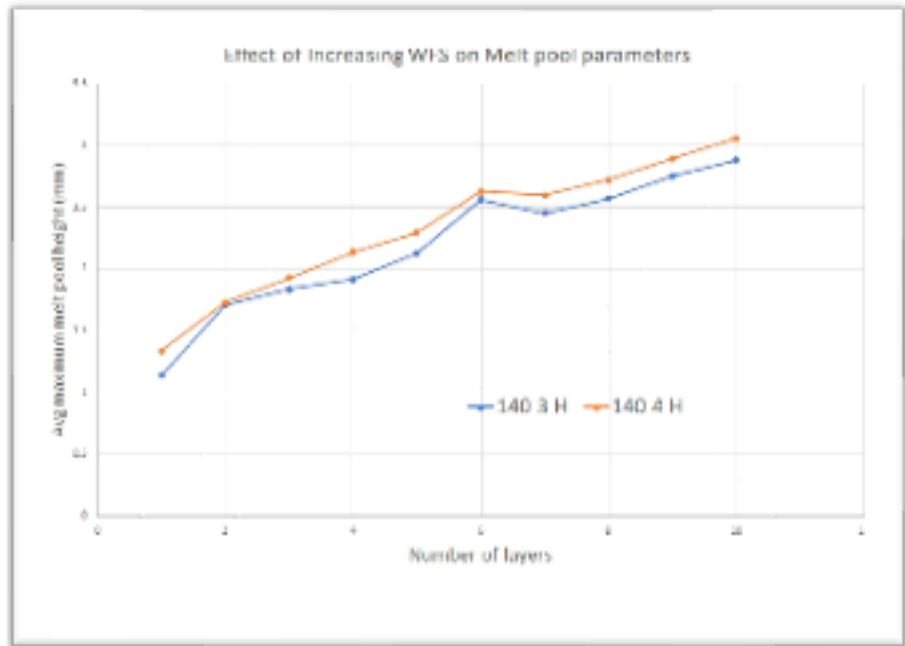


Fig. 4.15 Melt pool height with WFS increased from 3 to 4 at 140A current

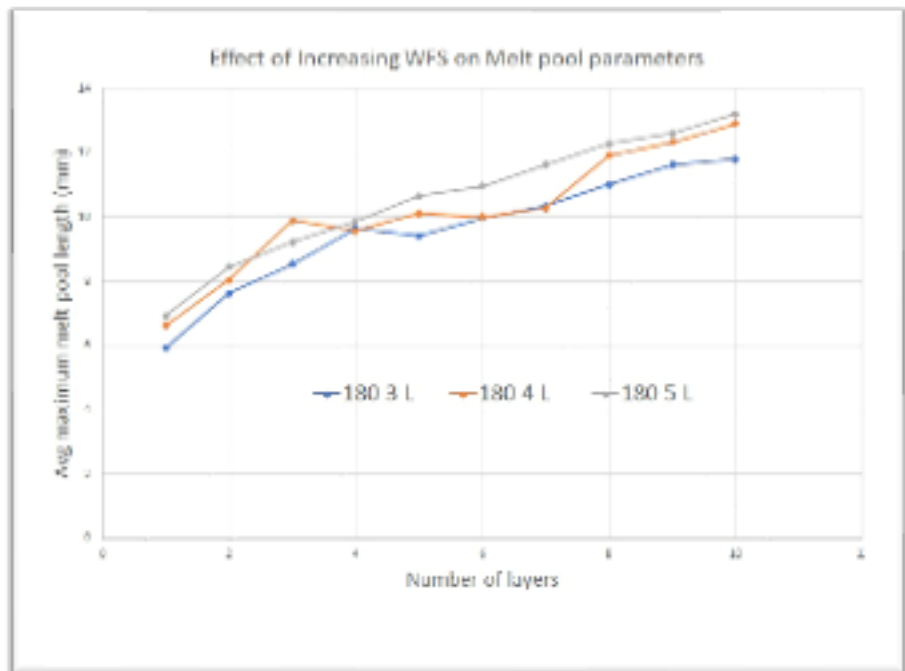


Fig. 4.16 Melt pool length with WFS increased from 3 to 5 at 180A current

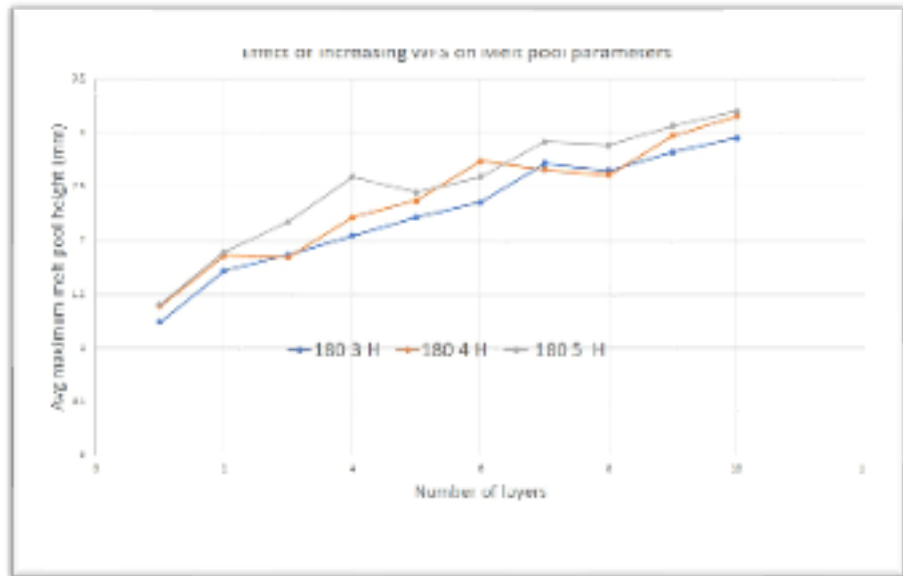


Fig. 4.17 Melt pool height with WFS increased from 3 to 5 at 180A current

4.1.3 Deposited layer height variations with successive layers for different deposition conditions

When the thickness of the deposited layer was observed at a constant current for successive layers then it showed the decreasing tendency in deposited layer height with successive layers even when the melt pool height was increasing with successive layers. This can be reconfirmed with the cross-sectional image of the specimen that the width at the root is lower compared to the top layer widths, with the succeeding layers the spread of metal is increasing.

The possible explanation for such decreasing tendency could be as the number of layers are increased then the melt pool size also increases and the arc pressure causes the molten metal to spread sidewise which causes the deposited layer height to decrease. The larger the melt pool size more the spread of molten metal takes place causing a further decrease in deposited layer thickness.

Variation of deposited layer height with the successive layers can be seen in the graph shown in Fig 4.18

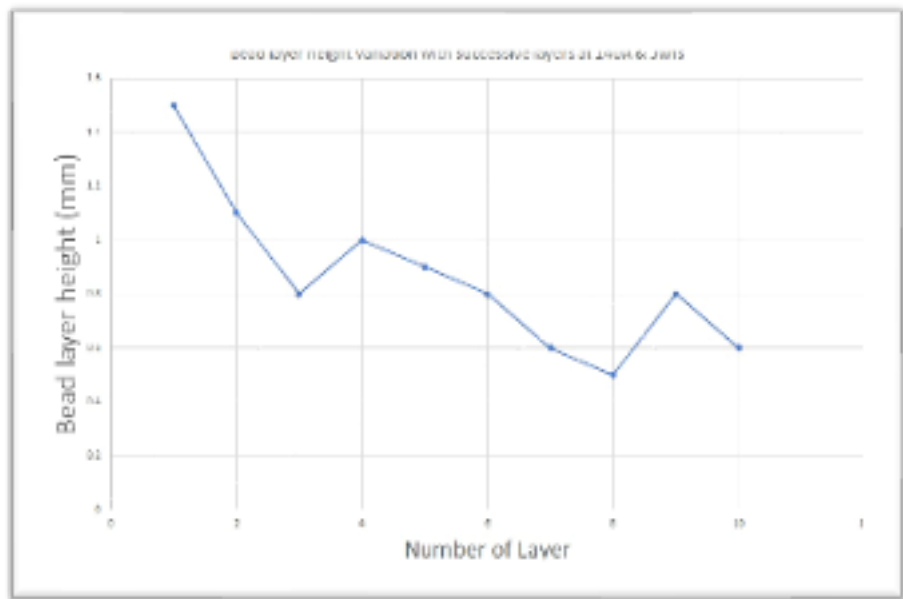


Fig. 4.18 Variation of deposited layer height with successive layers at 140A & 3 WFS

With the increase in the WFS since there was more material deposited per unit length thus, the deposited layer height was decreasing with successive layers but was still greater than the deposition that took place at lower WFS. The graph in figure 4.19 shows the effect of increased WFS at 140A current.

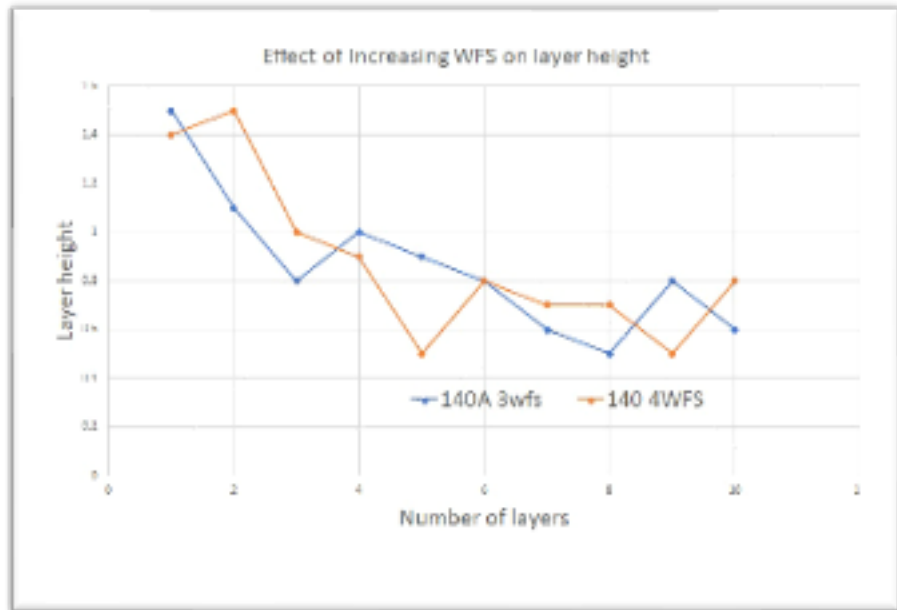


Fig. 4.19 Effect of increasing WFS from 3 to 4 m/min at 140 A current on bead layer height

With the increase in the current, the deposited layer height decreased, keeping the other parameters constant. The observed result could be explained by the same reason that as the current increased then the input energy increased causing the melt pool size to increase, increase in melt pool size was pushed by arc pressure causing the molten metal to be spread sidewise causing the further decrease in the deposited layer height. The deposited layer height was still showing decreasing tendency with successive layers but still, it was less than the layers deposited at a lower current value.

The graph in Fig. 4.20 shows the effect of an increase in current on deposited layer height.

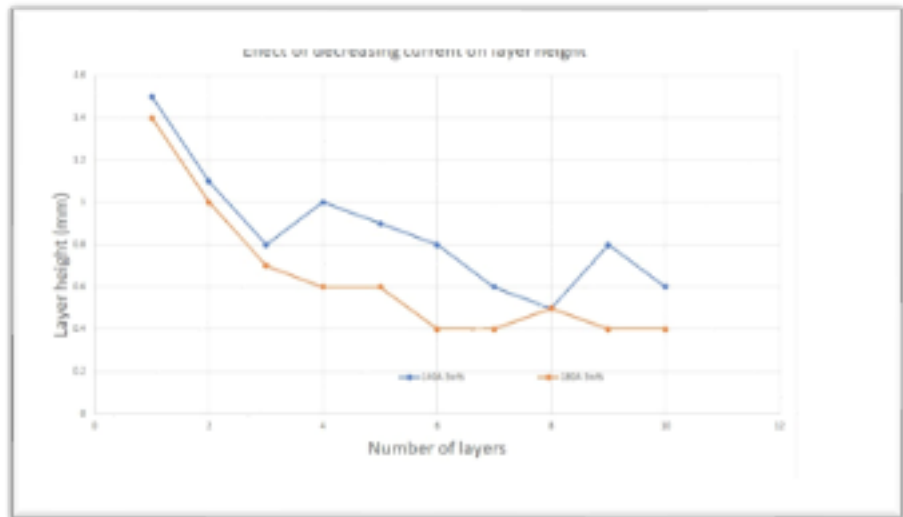


Fig. 4.20 Effect of increasing current from 140 to 180 A at 3 WFS on bead layer height

4.1.4 Cross-sectional analysis for different deposition conditions

The effect of changing current and WFS on bead cross-section was studied and observation was found that with an increase in WFS average bead width increased and average bead height also increased because of more metal deposition per unit area. Also, with an increase in current average bead width increased and average bead height decreased because no additional material is deposited per unit length but only the molten layer got spread more for higher currents Fig. 2.21 shows the cross-sections at different current and WFS values & Table 5 shows the effect of current and WFS on bead cross-sectional parameters, Fig 4.22 shows the bar chart of bead parameters variation with WFS and current.

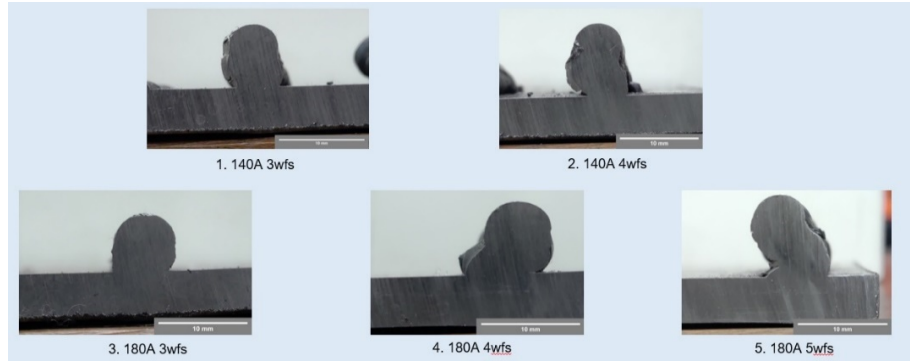


Fig. 4.21 Cross-section images at different deposition parameters at 200 mm/min travel speed

Table 5

	140 A 3wfs	140 A 4wfs	180 A 3wfs	180 A 4wfs	180 A 5wfs
Maximum Specimen Height (H)	7.415	9.215	6.416	7.207	9.295
Maximum Specimen Width (W)	6.247	6.664	7.050	8.023	7.453
Bead Width At Root	4.940	4.861	6.172	7.089	6.841
Average Cross-section Area (A)	38.868	52.772	39.020	47.640	56.494
Average Width (A/H)	5.241	5.726	6.081	6.610	6.077
Average Layer Thickness (A/n)	0.742	0.922	0.642	0.721	0.930

Table 6 Effect of current and WFS on bead cross-sectional parameters

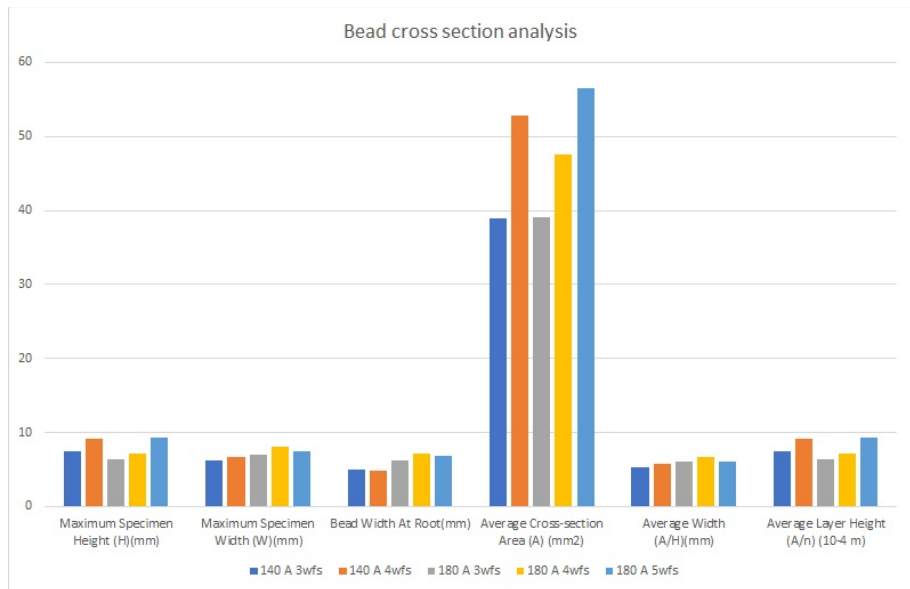


Fig. 4.22 Bar chart showing the Effect of current and WFS on bead cross-sectional parameters

4.2 Observations for constant current DWF WAAM

4.2.1 Melt pool diagrams for different deposition conditions

Similar to the SWF WAAM process in the DWF WAAM process also melt pool size increases with successive layers for constant current deposition. The increasing trend can be explained with the same reason as in SWF WAAM that melt pool length and melt pool height show an increasing trend with successive layers. Since at the initial layers the layer is deposited on the substrate plate or close to it thus the thermal conductive resistance is very less the heat loss rate is very high thus the majority of the heat gets lost through the substrate plate thus melt pool size is less initially but as the number of layers is increased then the distance of deposited layer with the substrate plate increases thus thermal conductive resistance gets increased each layer thus heat dissipation rate through conduction decreases with succeeding layers causing more heat to get accumulated in the melt pool zone itself thus melt pool size increases with successive layers. With the increase in the number of layers convective and radiative heat resistance gets decreased but the conductive heat resistance dominates over these 2 heat resistances thus there is not much effect of it in the initial deposition stages.

Melt pool of DWF WAAM was observed at 170 A current at 200 mm/min travel speed and a total of 3 m/min, SOD 4 mm, Electrode vertex angle 45°, gas flow rate 10 l/min deposition length 60 mm, substrate material AISI 1020 sheet 5 mm used and the images of observed melt pool are as shown in Fig. 21, total 22 layers have been deposited and it can be observed with melt pool images that with successive layers melt pool length and melt pool height increased. Fig 4.23 shows the melt pool images of the double wire feed deposition process and Fig. 4.24 shows Sample images of DWF deposited specimen at a total of 4.8 WFS.

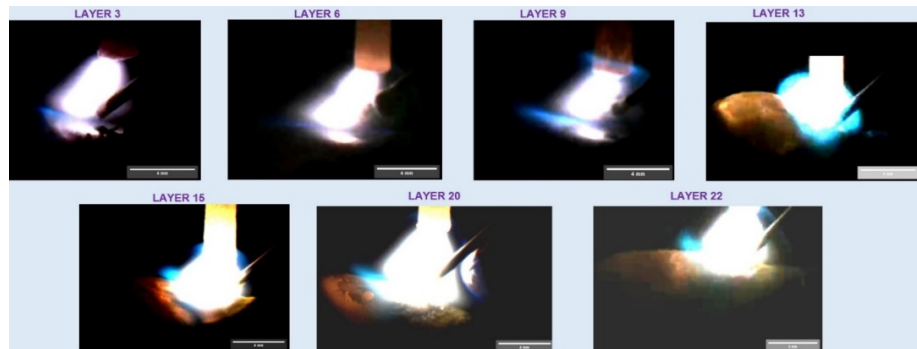


Fig. 4.23 Melt pool images for DWF WAAM at 170 A current, a total of 3 WFS, and 200 mm/min deposition speed



Fig. 4.24 Sample images of DWF deposited specimen at a total of 4.8 WFS

SWF WAAM was also deposited at a similar deposition condition to compare the melt pool parameter of DWF WAAM with SWF WAAM and it was observed that for a similar deposition condition melt pool length and height are marginally bigger for DWF WAAM compared to SWF WAAM. A total of 12 layers were deposited for SWF WAAM at the same deposition parameter.

Fig 4.25 & 4.26 shows the variation of melt pool length and height for both SWF WAAM and DWF WAAM.



Fig. 4.25 Melt pool size at 170 A and 3 WFS for SWF WAAM

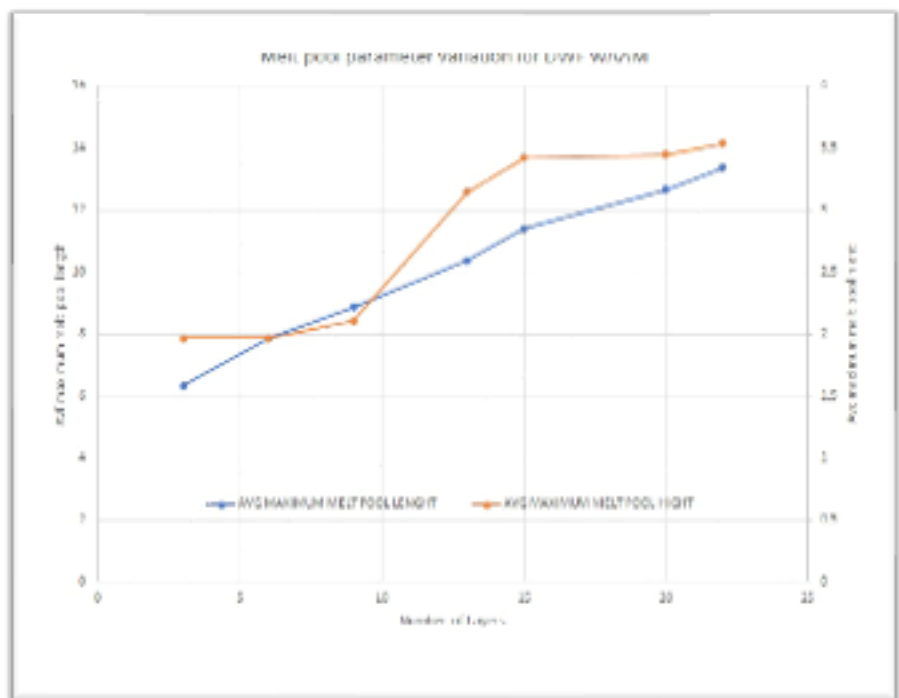


Fig. 4.26 Melt pool size at 170 A and 3 WFS for DWF WAAM

4.2.2 Deposited layer height variations with successive layers for different deposition conditions for DWF WAAM

Similar to the SWF WAAM process when the height of the deposited layer was observed at a constant current for successive layers then it also showed the decreasing tendency in deposited layer height with successive layers even when the melt pool height was increasing with successive layers. This can be reconfirmed with the cross-sectional image of the specimen that the width at the root is lower compared to the top layer widths, with the succeeding layers the spread of metal is increasing.

The possible explanation for such decreasing tendency could be as the number of layers are increased then the melt pool size also increases and the arc pressure causes the molten metal to spread sidewise which causes the deposited layer height to decrease. The larger the melt pool size more the spread of molten metal takes place causing a further decrease in the deposited layer height.

Variation of deposited layer height with the successive layers can be seen in the graph shown in Fig 4.27.

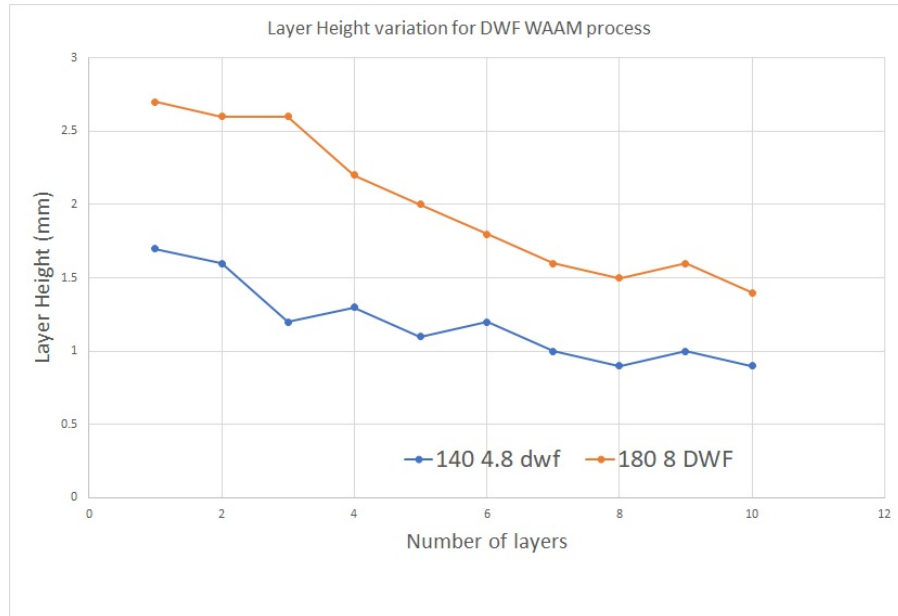


Fig. 4.27 Layer height for deposition at 140A 4.8 WFS & 180A 8 WFS

4.2.3 Comparison of deposition rate between SWF WAAM & DWF WAAM

It was observed that for the SWF WAAM process done at 140 A current and 200 mm/min travel speed then maximum optimized WFS was 3.5 m/min which is 989.982 mm³/min for a wire diameter of 0.6 mm and for the same deposition condition when the deposition was done for DWF WAAM process then optimized WFS was coming out to be 5 m/min which is 1414.26 mm³/min for wire diameter 0.6 mm.

Similarly for the SWF WAAM process done at 180 A current and 200 mm/min travel speed then maximum optimized WFS was 5 m/min which is 1414.26 mm³/min for a wire diameter of 0.6 mm and for the same deposition condition when the deposition was done for DWF WAAM process then optimized WFS was coming out to be 8 m/min which is 2262.816 mm³/min for wire diameter 0.6 mm.

Thus, a total of 37.14 % of increment in deposition rate was observed for the 140A current and a 60% of increment in deposition rate was observed in the 180A current. The increase in deposition rate was obtained without increasing the input power which confirms that the

deposition rate can be increased using the DWF without increasing the input energy.

This also solidifies our given reason for the improvement in the deposition rate which was that the temperature and power distribution of arc between electrode and melt pool is bell-shaped and wire that is fed covers very less area of arc zone. So a substantial amount of energy goes to the melt pool which can be utilized for second wire deposition. Table 6 shows the comparison of deposition between SWF WAAM and DWF WAAM and Fig. 4.28 shows the bar chart of the comparison of Deposition rate comparison for SWF &DWF at 140A current & Fig. 4.29 shows the bar chart of the comparison of Deposition rate comparison for SWF &DWF at 180A current

Table 6

Sr. No.	Current (A)	Travel speed (mm/min)	Maximum WFS for SWF (m/min)	Maximum material deposition rate for SWF (mm ³ /min)	Maximum WFS for DWF (m/min)	Maximum material deposition rate for DWF (mm ³ /min)	Percentage of increment in deposition rate for DWF wrt SWF
1	140	200	3.5	989.982	5	1414.26	37.14
2	180	200	5	1414.26	8	2262.816	60

Table 6 comparison of deposition between SWF WAAM and DWF WAAM

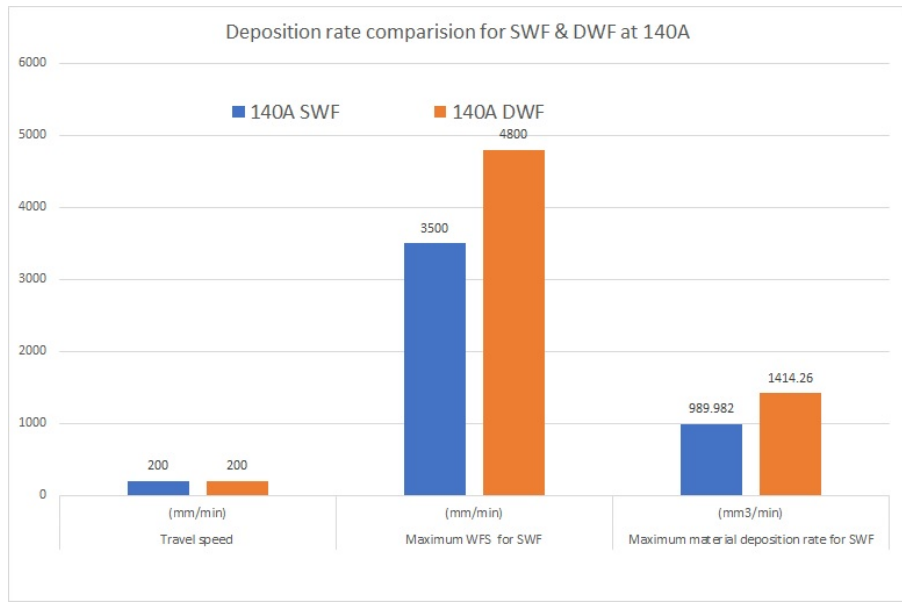


Fig. 4.28 Deposition rate comparison for SWF & DWF at 140A current



Fig. 4.29 Deposition rate comparison for SWF & DWF at 180A current

4.3 Observations for decreasing current in succeeding layers for SWF WAAM

4.3.1 Melt pool diagrams for decreasing current in succeeding layers for SWF WAAM

Controlling the bead thickness has been a challenging task for the WAAM process thus many efforts have been made to control it. We have also tried to control it by decreasing the current at each successive layer and it has shown a promising result for controlling the deposited layer thickness.

It was observed that when the deposition was done with the decreasing current in each layer then initially the melt pool length and height increased then became steady and in the latter most layer it decreased a bit. This observation could be explained by combining the effect of change in 2 parameters simultaneously. As with succeeding layers the thermal resistance increases which tends to increase the melt pool size while with each layer since the current has been decreased thus reducing heat input in succeeding layers which tend to decrease the melt pool size. Since both of these parameters tend to oppose each other thus initially since the thermal resistance dominates thus little increment can be seen in melt pool size but after some layers, both parameters dominate equally thus steady melt pool size is observed, and at later most layers since the effect of thermal resistance is not increased that significantly thus reduction in heat input dominates thus melt pool size decreases.

Initially at first layer current was taken 210A and then with each layer current was reduced by 10A, WFS was taken at 4 m/min and the

observed melt pool has been shown in the Fig 4.30 and Fig 4.31 shows the graphical representation of the melt pool length and height with successive layers for decreasing current in successive layers.

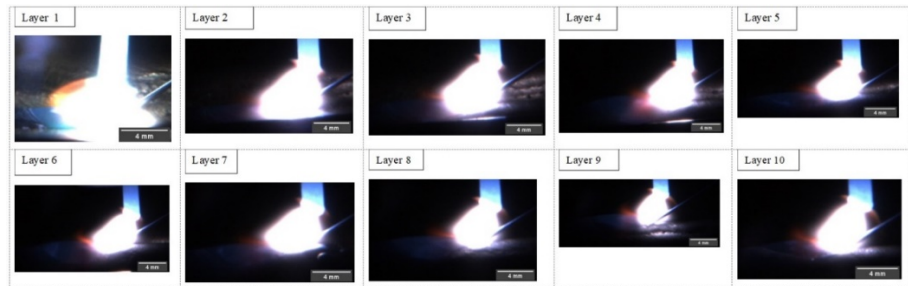


Fig. 4.30 Melt pool diagram for decreasing current from 210A to 120A current at 4 m/min WFS

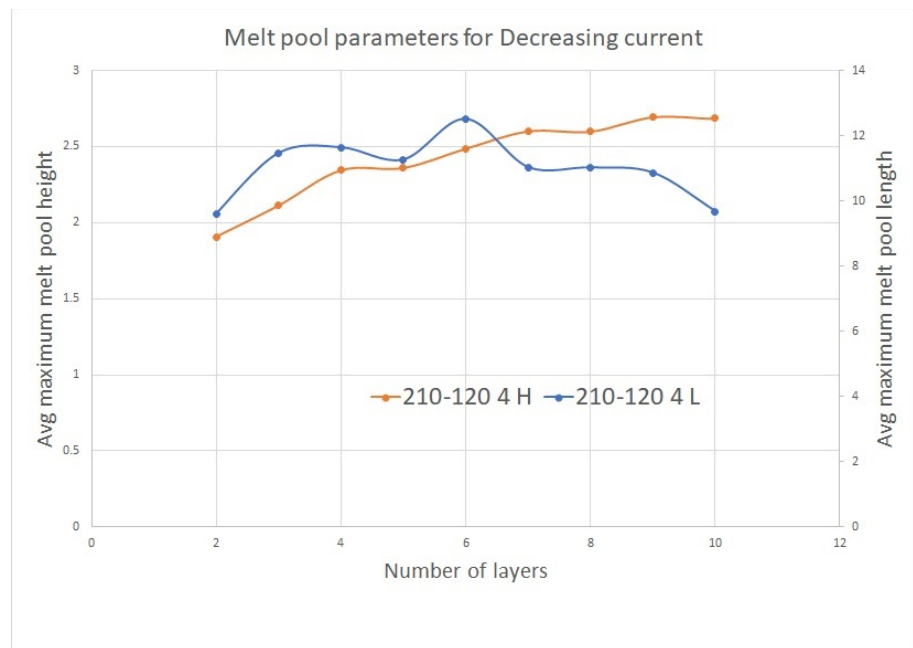


Fig. 4.31 Melt pool length and height variation for decreasing successive layer current at 4 WFS

4.3.2 Deposited layer height variations with successive layers for decreasing successive layer current deposition

When the height of deposited layer was observed at decreasing successive layer current, for successive layers then it showed steady deposited layer height with successive layers initially and decreased a bit in latter most stages.

The possible explanation for such steady deposited layer height could be as the number of layers is increased then the melt pool size initially increases and then becomes steady which does not let the arc pressure cause the molten metal to spread sidewise to that much extent, which ultimately leads the deposited layer height to become steady.

Table 7 shows the deposited layer height observed and current used at each layer which confirms the steadiness of the deposited layer height and Fig 4.32 shows a graphical representation of the deposited layer height with successive layers.

Layers	1	2	3	4	5	6	7	8	9	10
Current	18	17	17	16	16	15	14	13	12	11
(A) Ex. 1, 3WFS	0	5	0	5	0	0	0	0	0	0
Thickne ss (mm)	1. 1	1	1	0. 9	0. 8	0. 6	1. 3	1	0. 8	0. 9
Current	21	20	19	18	17	16	15	14	13	12
(A) Ex. 2, 4WFS	0	0	0	0	0	0	0	0	0	0
Thickne ss (mm)	1. 4	1. 3	1. 1	0. 8	1. 3	1. 2	1	1	1. 4	1

Table 7 Deposited layer height variation for decreasing successive layer current

Table 7

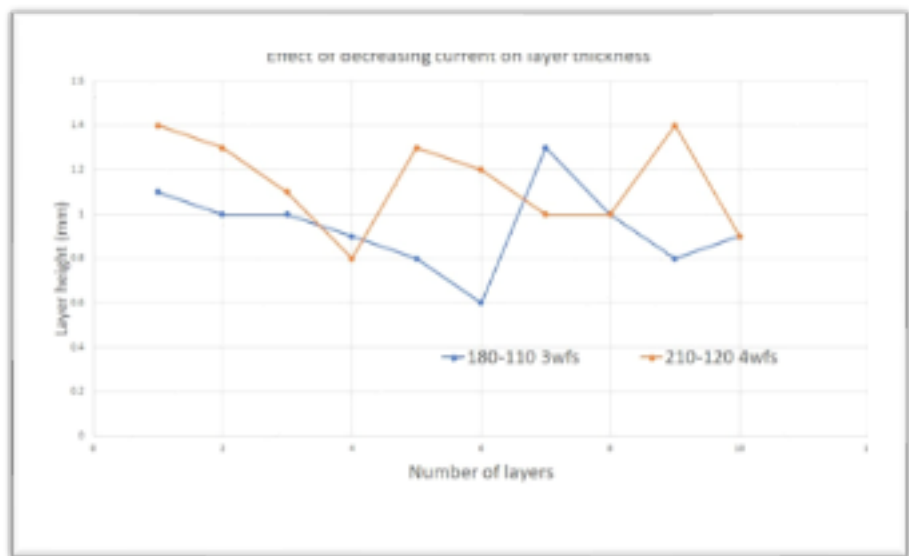


Fig. 4.32 Deposited layer height variation for decreasing successive layer current

Since constant current at each layer gives the decreasing trend of deposited layer height and decreasing successive layer current shows steady deposited layer thickness thus decreasing successive layer current can be used to control the layer height.

Fig 4.33 & 4.34 shows the comparison of deposited layer height between deposition at constant successive layer current and deposition at decreasing successive layer current.

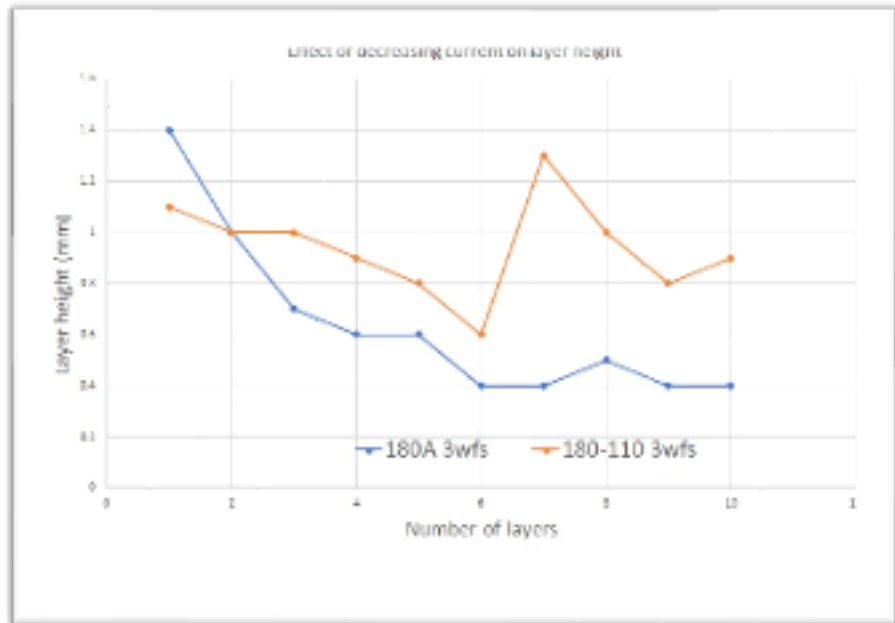


Fig. 4.33 Deposited layer height comparison between constant & decreasing successive layer current at 3 WFS

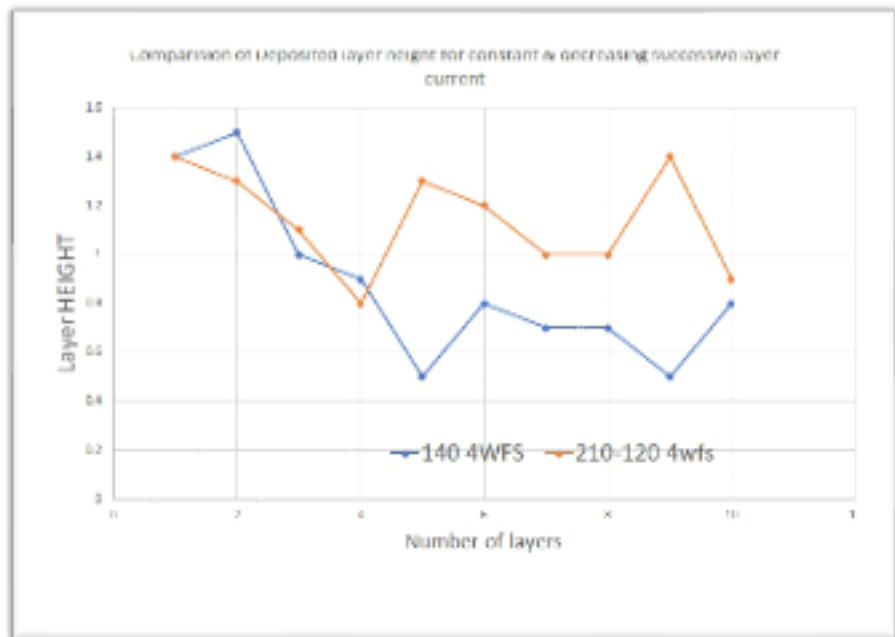


Fig. 4.34 Deposited layer height comparison between constant & decreasing successive layer current at 4 WFS

Chapter 5: Conclusions and Future Scope

5.1 Conclusions

- With successive layers for constant current SWF WAAM process, the length, and height of the melt pool increase.
- With the increase in WFS and current, melt pool length and height show an increasing trend.
- Even though the melt pool parameters increase with successive layers but bead layer height shows a decreasing trend with successive layers for the SWF WAAM process.
- With the increase in WFS the deposited layer height increases and with an increase in current deposited layer height decreases for the SWF WAAM process.
- Melt pool length and height for DWF WAAM show a similar trend as SWF WAAM process but are slightly higher than SWF WAAM for the same deposition condition.
- Increment in deposition rate of **37.14%** for 140A current and **60%** for 180A current was observed for DWF WAAM process compared to SWF WAAM process without increasing the input energy and without altering the deposition parameters.

- With decreasing current in successive layers melt pool length first increases then stabilizes then again decreases while melt pool height first increases then stabilizes but not decreases at latter most layers.
- Bead layer height decreases with successive layers at constant current but it stabilizes for decreasing current in successive layers.
- With the increase in current and increase in WFS bead width increases.
- It was observed that layer height was correlated with melt pool size.

5.2 Future scope

- Different melt pool size controlling methodologies can be used which will further control the layer thickness and provide steadiness in the deposited layer parameters thus more uniform properties.
- On WAAM, the control system can be used to produce complicated 3D items with minimal defects
- The correlation between the layer thickness and current with the succeeding layer can be made to control the layer thickness.
- Using the hot wire feeders further increase in deposition rate can be expected for both SWF and DWF WAAM processes.

References

1. Frazier, W.E. Metal Additive Manufacturing: A Review. *J. of Materi Eng and Perform* 23, 1917–1928 (2014).
<https://doi.org/10.1007/s11665-014-0958-z>
2. S. W. Williams, F. Martina, A. C. Addison, J. Ding, G. Pardal & P. Colegrove (2016) Wire + Arc Additive Manufacturing, *Materials Science and Technology*, 32:7, 641-647, DOI: 10.1179/1743284715Y.0000000073
(<https://doi.org/10.1179/1743284715Y.0000000073>)
3. Sergio Ríos, Paul A. Colegrove, Filomeno Martina, Stewart W. Williams, Analytical process model for wire + arc additive manufacturing, *Additive Manufacturing*, Volume 21, 2018, Pages 651-657, ISSN 2214-8604,
<https://doi.org/10.1016/j.addma.2018.04.003>
4. Md.R.U. Ahsan, A.N.M. Tanvir, Gi-Jeong Seo, Brian Bates, Wayne Hawkins, Chanhoo Lee, P.K. Liaw, Mark Noakes, Andrzej Nycz, Duck Bong Kim, Heat-treatment effects on a bimetallic additively-manufactured structure (BAMS) of the

- low-carbon steel and austenitic-stainless steel, Additive Manufacturing, Volume 32, 2020, 101036, ISSN 2214-8604, <https://doi.org/10.1016/j.addma.2020.101036>
5. beuth et al. ,2013, mechanical engineering, additive manufacturing process mapping direct metal deposition melt pool geometry microstructure, <http://dx.doi.org/10.26153/tsw/15590>
 6. Yuehai Feng, Bin Zhan, Jie He, Kehong Wang, The double-wire feed and plasma arc additive manufacturing process for deposition in Cr-Ni stainless steel, Journal of Materials Processing Technology, Volume 259, 2018, Pages 206-215, ISSN 0924-0136, <https://doi.org/10.1016/j.jmatprotec.2018.04.040>
 7. A B Murphy et al Modelling of thermal plasmas for arc welding: the role of the shielding gas properties and of metal vapour2009 J. Phys. D: Appl. Phys. 42 194006
 8. O. Diegel. "Additive Manufacturing", engineering, Elsevier BV, 2014
 9. Mahamani, A.; Kumar, P.; Ismail, K.; Jawahar, S.; Chiranjeevi Reddy, T.; Vijayasai, T.; Venkata Phaneendra, T.; Uday sankar, V.; Gopi chandu, V., 2018, Mono and multi-response optimization of 3D printer parameters to attain improved hardness and surface roughness, <http://doi.org/10.1088/1757899X/390/1/012100>
 10. Kumar, Ashish; Maji, Kuntal,2020, Selection of Process Parameters for Near-Net Shape Deposition in Wire Arc Additive Manufacturing by Genetic Algorithm, <http://doi.org/10.1007/s11665-020-04847-1>
 11. Leng, Xuedong; Zhang, Gwangju; Wu, Lin, 2006, The characteristic of twin- electrode TIG coupling arc pressure , <http://doi.org/10.1088/0022-3727/39/6/017>
 12. Ahmet Suat Yildiz^{1,2} & Kemal Davut^{3,4} & Barış Koc¹ & Oguzhan Yilmaz²,2020, Wire arc additive manufacturing of high-strength low alloy steels: study of process parameters and

their influence on the bead geometry and mechanical characteristics, The International Journal of Advanced Manufacturing Technology, <http://doi.org/10.1007/500170-020-05482-9>

13. Sun, Z., Guo, W., & Li, L. (2020). In-process measurement of melt pool cross-sectional geometry and grain orientation in a laser directed energy deposition additive manufacturing process. Optics and Laser Technology, 129, 106280. <https://doi.org/10.1016/j.optlastec.2020.106280>
14. Soylemez, Emre Can Beuth, Jack L., 2010, Controlling Melt Pool Dimensions Over a Wide Range of Material Deposition Rates in Electron Beam Additive Manufacturing, <http://dx.doi.org/10.26153/tsw/15221>
15. Malcolm Dinovitzer, Xiaohu Chen, Jeremy Laliberte, Xiao Huang, Hanspeter Frei, Effect of wire and arc additive manufacturing (WAAM) process parameters on bead geometry and microstructure, Additive Manufacturing, Volume 26, 2019, Pages 138-146, ISSN 2214-8604, <https://doi.org/10.1016/j.addma.2018.12.013>
16. Filippo Montevercchi, Giuseppe Venturini, Antonio Scippa, Gianni Campatelli, Finite Element Modelling of Wire-arc-additive manufacturing Process, Procedia CIRP, Volume 55, 2016, Pages 109-114, ISSN 2212-8271, <https://doi.org/10.1016/j.procir.2016.08.024>